Option Pricing for Continuous-Time Log-Normal Mixtures

Joakim Björnander
joakim.bjornander@gmail.com

Supervisor:
Prof. Christer Borell

May 30, 2012

Department of Mathematical Sciences
Division of Mathematics
Chalmers University of Technology and University of Gothenburg
SE-41296 Gothenburg, Sweden

Abstract

In this thesis we study the log-normal mixture option pricing model proposed by Brigo and Mercurio [1]. This model is of particular interest since it is an analytically tractable generalization of the Black-Scholes option pricing model, but essentially of the same degree of complexity when it comes to computing option prices and hedging.

Therefore, if the Brigo-Mercurio model proved to be better in terms of hedging it would be preferable to the Black-Scholes model from a market practitioner's point of view.

In the latter part of this thesis we will investigate various methods of hedging and present the results.

Acknowledgements

First and foremost I would like to thank my supervisor Prof. Christer Borell for his guidance. Christer's never-tiring reading of the manuscripts together with his insightful comments have been very helpful. It has been a privilege to partake of Christer's immense knowledge and I have learned a lot from our conversations, not only about mathematics.

I would also like to thank my beloved Anna for constantly supporting me and listening to my dilemmas. And not to forget all my friends at the Mathematics department, in particular Oskar, Sandra, and Ivar, for making these five years of study a pleasure.

Contents

Chapter 1

Introduction

In this thesis we will investigate the Brigo-Mercurio log-normal mixture model [1], which is a generalization of the the famous Black-Scholes option pricing model. We begin by highlighting some of the drawbacks in the Black-Scholes model and explain intuitively the idea behind the Brigo-Mercurio model and why it could eventually be more suitable to model the market.

The Black-Scholes model is based on several underlying assumptions about the market. The main assumption is that the underlying price process $S = (S(t))_{t\geq 0}$ is governed by a geometric Brownian motion (GBM). This means by definition that the log-price process $(\ln S(t))_{t\geq 0}$ is a Brownian motion with drift or equivalently that

$$S(t) = S(0)e^{(\mu - \frac{\sigma^2}{2})t + \sigma W(t)}, \quad t \geq 0 \tag{1.1}$$

where $(W(t))_{t\geq 0}$ as a standard Brownian motion, $\mu \in \mathbb{R}$, and $\sigma > 0$ are fixed parameters and $S(0) > 0$. In particular the log-returns are normally distributed, since for $u \leq t$ we get

$$\ln\left(\frac{S(t)}{S(u)}\right) = (\mu - \frac{\sigma^2}{2})(t-u) + \sigma(W(t) - W(u))$$

which implies that

$$\ln\left(\frac{S(t)}{S(u)}\right) \in N\left((\mu - \frac{\sigma^2}{2})(t-u), \sigma^2(t-u)\right).$$

Also, as a direct consequence of the definition of Brownian motion it follows that the log-returns on non-overlapping time periods are independent i.e.

$$\ln\left(\frac{S(t_2)}{S(t_1)}\right) \quad \text{and} \quad \ln\left(\frac{S(t_4)}{S(t_3)}\right)$$

are independent if $0 \leq t_1 \leq t_2 \leq t_3 \leq t_4$. When working with real market data it becomes apparent that these two properties do not describe the real

market perfectly. This will be demonstrated in this introduction by using market data.

Throughout this thesis the price process S consists of daily closing prices from the Euro Stoxx 50 Index [2] and whenever we refer to the *real* stock price we mean this index. The Index consists of 50 stocks from 12 different Eurozone countries and is described in more detail in Section 6.1. In Figure 1.1 we plot the Euro Stoxx 50 index over a 2 month period.

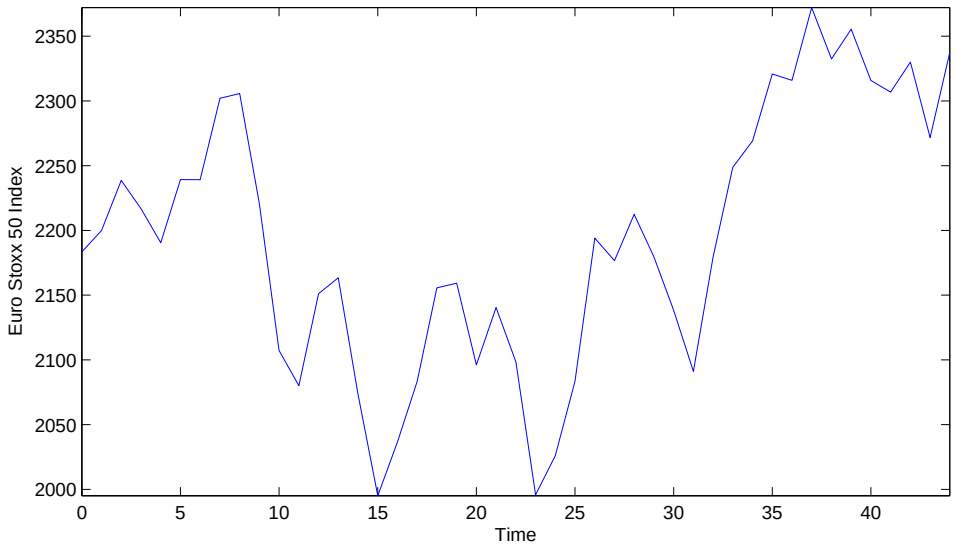

Figure 1.1: A plot of the Euro Stoxx 50 Index over the 2 month period 2011-08-22 to 2011-10-21.

Moreover, we will consider European call options on S. Here recall that a European call option on S with strike price K and time of maturity T pays the amount

$$\max(0, S(T) - K)$$

to its owner at time of maturity T. In the sequel, whenever we speak of a call option we mean a European call option.

For a bank or institution it is often desirable to be able to sell a call option (or other options) without taking too high risk – to hedge the call option. In the Black-Scholes model it is possible to perfectly hedge a call option by trading only in the underlying asset S and the bond (a money market account). This however, requires the hedging portfolio to be rebalanced continuously in time. In practice, of course, it is impossible to trade in continuous time and this gives rise to what we call hedging error.

The parameters μ and σ in (1.1) are called drift and volatility, respectively. If $\mu \geq \sigma^2/2$ it means that the price process has a tendency to increase

and vice versa if $\mu < \sigma^2/2$. By statistical means the drift parameter μ is impossible to estimate with a small enough variance and is ultimately a matter of the investors' prospects of the future. One of the greatest results in the Black-Scholes option pricing theory is that the option prices are independent of μ. Moreover, it is possible to change to an equivalent measure under which the parameter μ is replaced by the risk-free rate r. This measure is called the risk-neutral measure.

1.1 The Gaussian Assumption

As we already noted, the Black-Scholes model implies that the log-returns of the price process are normally distributed. In this section we will see that this assumption does not reflect the market very well. We will also see how a mixture of normal densities might eventually be a better way to model the log-returns.

Using the real stock index prices we can construct an empirical probability density histogram of daily log-return over a 12-month period. With daily log-returns we mean

$$X_n = \ln\left(\frac{S_n}{S_{n-1}}\right), \quad n = 1, ..., N.$$

where S_n denotes the real stock price at the end of the n:th business day. Figure 1.2 is such a histogram together with normal probability density plot that has been fitted to empirical log-returns. The parameters of the normal density were estimated using Matlab's function `normfit`. We can clearly see that the normal assumption is not perfect. Note, for example, that the empirical density has a greater peak around the mean and a bit heavier tails than the normal density.

However, as we will see, the normal assumption tends to be more suitable if we consider shorter time periods. In Figure 1.3 we have an empirical probability density histogram of daily log-returns over a 2 month period together with a fitted normal density plot. It is closer to being normal compared with the 12-month period case in Figure 1.2. One possible explanation for this may be that it is more likely that there will occur extreme events over a longer than over a shorter period of time.

The main purpose of this thesis is to investigate a generalization by Brigo and Mercurio [1] of the Black-Scholes model. In the Brigo-Mercurio model the density of the price process, at a fixed time point, relative to the risk-neutral measure will be a mixture of log-normal densities i.e. a convex combination of log-normal densities. In Chapter 2 we will demonstrate and see the benefits of a mixture of log-normal densities which is of central importance in this thesis.

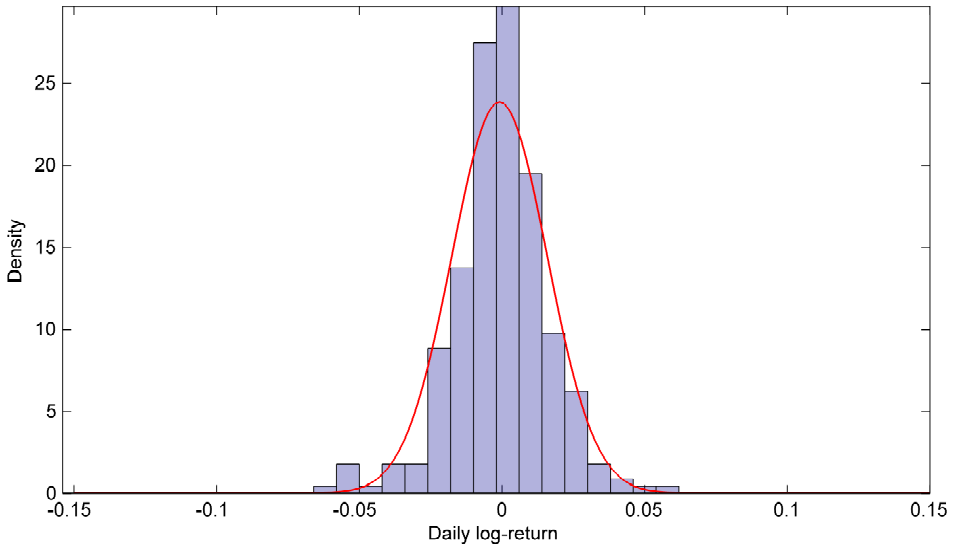

Figure 1.2: A probability density histogram of daily log-returns using index data for the 12 month period 2010-10-18 to 2011-11-18. Here displayed together with a fitted normal distribution.

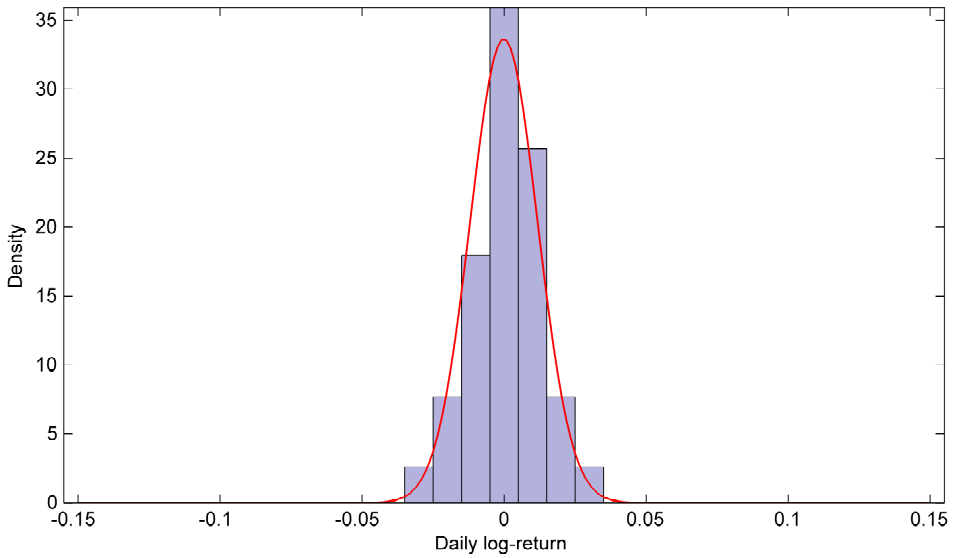

Figure 1.3: A probability density histogram of daily log-returns using index data for the 2 month period 2010-10-18 to 2010-12-18. Here displayed together with a fitted normal distribution.

As a demonstration of how we can benefit from mixture densities we will mix normal densities and see that we get a better fit to the empirical distribution in Figure 1.2 compared to only one normal density.

Recall that the density function of the normal distribution with mean μ and variance σ^2 is

$$\varphi(x;\mu,\sigma) = \frac{1}{\sigma\sqrt{2\pi}} e^{-\frac{(x-\mu)^2}{2\sigma^2}}.$$

A mixture of two normal densities has the following form

$$\begin{cases} \lambda_1\varphi(x;\mu_1,\sigma_1) + \lambda_2\varphi(x;\mu_2,\sigma_2), \\ \lambda_1 + \lambda_2 = 1,\ \lambda_1 \geq 0, \lambda_2 \geq 0. \end{cases}$$

By mixing two normal densities we can achieve a density which has got higher peaks around the mean and heavier tails. This is illustrated in Figure 1.4 where we have a normal density and a mixture of two normal densities. They have both been fitted to the empirical data over the same 12-month period data used in Figure 1.2. The mixture density was fitted using Matlab's function `gmdistribution.fit`. The normal density has mean 0 and standard deviation 0.0167 and the mixture density is a mixture of a normal density with mean 0 and standard deviation 0.0103 and normal density with mean 0 and standard deviation 0.0233 where the weights are 0.61 on the first one and 0.39 on the second one. This is summarized in Table 1.1.

	Normal	Mixture	
μ	0	0	0
σ	0.0167	0.0103	0.0233
λ	1	0.61	0.39

Table 1.1: The densities used in Figure 1.4 and 1.5.

In Figure 1.5 we can see the densities from Figure 1.4 together with the empirical density. Clearly a mixture of two normal densities fits the empirical data much better and such a mixture of densities could eventually be more suitable to model the market compared to just one normal density. One can mix any number of normal densities and if we would use three we would get an even slightly better fit as can be seen in Figure 1.6. Using more than three normal densities the improvement is not very significant (and it will be increasingly difficult to fit it to data). Later, when we mix log-normal densities, a mixture of two or three normal densities will be enough for our applications.

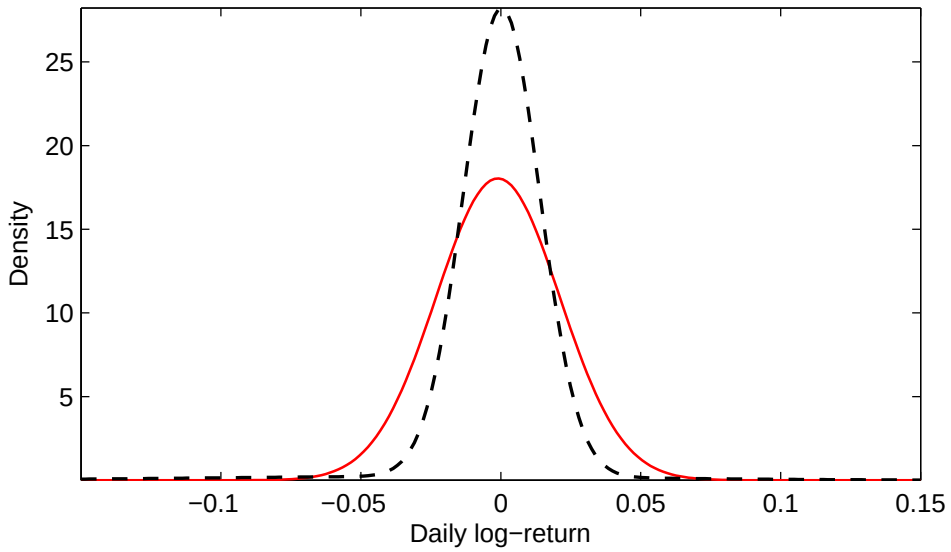

Figure 1.4: Comparison between a fitted normal distribution (solid line) and a fitted mixture of two normal densities (dashed line).

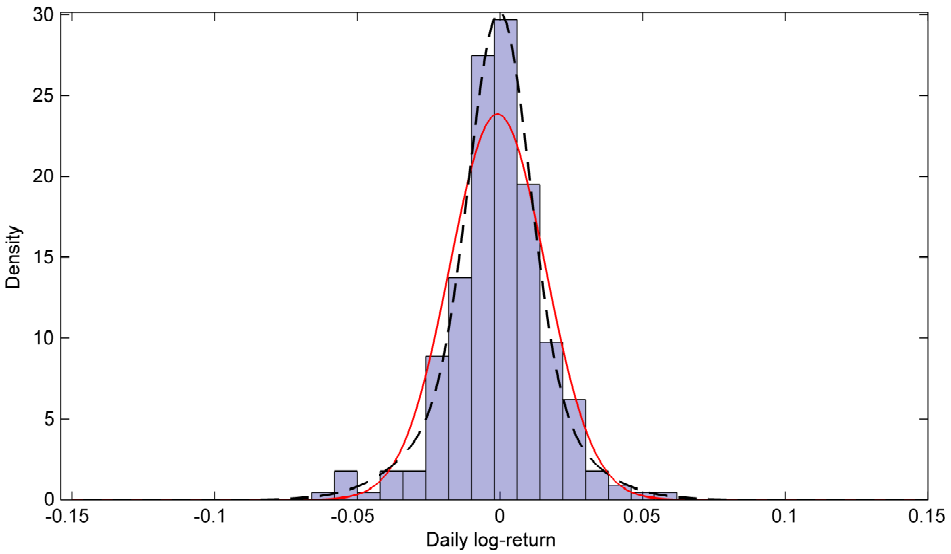

Figure 1.5: A probability density histogram of daily log-returns using index data for the 12 month period 2010-10-18 to 2011-11-18. The density histogram is displayed together with a fitted normal distribution (solid line) and a fitted mixture of two normal densities (dashed line).

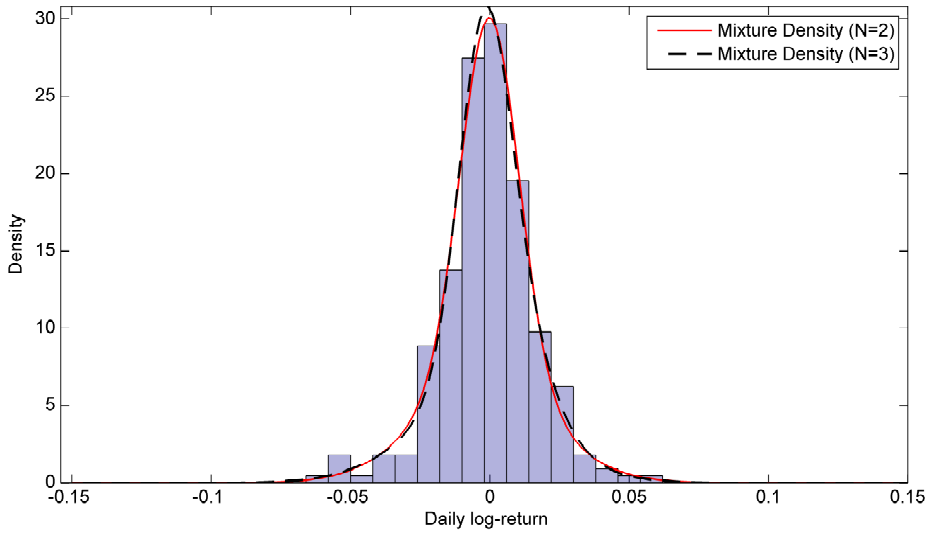

Figure 1.6: A probability density histogram of daily log-returns using index data for the 12 month period 2010-10-18 to 2011-11-18. The density histogram is displayed together with two mixtures of normal densities.

1.2 Independence

As mentioned above the real stock price process consists of daily quotes so we consider a time discretization $t_0 < t_1 < ... < t_N$ where each time point represents one day i.e. $t_i - t_{i-1} = 1$, $i = 1, ..., N$. Moreover, we introduce the following log-returns

$$X_n = \ln\left(\frac{S(t_n)}{S(t_{n-1})}\right), \quad n = 1, ..., N.$$

According to the geometric Brownian motion (GBM) assumption the log-returns $(X_n)_1^N$ are independent and normally distributed with mean $\mu - \sigma^2/2$ and variance σ^2. We will now test if it is likely that the observed market log-returns also stems from an i.i.d process.

We proceed in the fashion of Brockwell and Davis [3] and assume that $(Y_n)_{n=1}^N$ is an i.i.d. process with mean 0 and variance σ^2 and estimate the autocorrelation function (with time lag 1) by

$$\hat{\rho} = \frac{\sum_{n=1}^{N-1}\left(Y_n - \bar{Y}\right)\left(Y_{n+1} - \bar{Y}\right)}{\sum_{n=1}^{N}\left(Y_n - \bar{Y}\right)^2}$$

where

$$\bar{Y} = \frac{1}{n}\sum_{n=1}^{N} Y_n.$$

If we further assume some technical assumptions such as the existence of higher order moments of Y_n, $n = 1, ..., N$. Then according to Example 7.2.1 in [3] the sample autocorrelation function $\hat{\rho}$ is, for large N, asymptotically normally distributed with mean 0 and variance $1/N$. This implies that approximately 95% of the sample autocorrelations should lie in the confidence interval $[-1.96/\sqrt{N}, 1.96/\sqrt{N}]$. This can be used as a check to see if observed market log-returns are truely i.i.d.

We calculate the sample autocorrelation using our market daily stock prices over the period 2010-10-19 – 2011-11-18 i.e. $N = 238$. The sample autocorrelation is then -0.03 and a 95% confidence interval is $[-0.05, 0.05]$. Therefore we have no grounds for rejecting the hypothesis that (X_n) is an i.i.d. process at the 95% confidence level.

However, if we instead consider the process of squared log-returns

$$X_n^2 = \left(\ln \left(\frac{S(t_n)}{S(t_{n-1})} \right) \right)^2, \quad n = 1, ..., N$$

the GBM model implies that $(X_n^2)_1^N$ are still independent. But if we proceed as above and calculate the sample autocorrelation corresponding to the squared log-returns we get 0.20 which is significantly larger than zero and well outside the 95% confidence interval $[-0.05, 0.05]$. We can therefore reject the hypothesis that the squared log-returns is an i.i.d process.

1.3 Implied Volatility

The term volatility is often used in connection with assets as a measure of the amount of fluctuation and uncertainty there is in the future movements of the asset.

One major assumption in the Black-Scholes model is that the volatility of the underlying price process is constant. In this section we argue why constant volatility is not desirable in a market model and present a natural extension. If we think of the Black-Scholes call option price as a function of the volatility, then there exists a unique volatility so that the Black-Scholes price corresponds exactly to the market price of the call option. This specific volatility is widely known as the implied volatility and denoted by σ_{imp}.

If the Black-Scholes model was a perfect model for real stock prices, then the implied volatility would be constant for all fixed strikes and times to maturity. However, it does not take much investigation to realize that the implied volatility is in fact not constant. As an example to demonstrate this see Figure 1.7 where we have plotted the daily implied volatility of a 2-month European call option on the Euro Stoxx 50 Index. It is clear that the implied volatility is not constant and thus using a constant volatility model might lead to a significant hedging error.

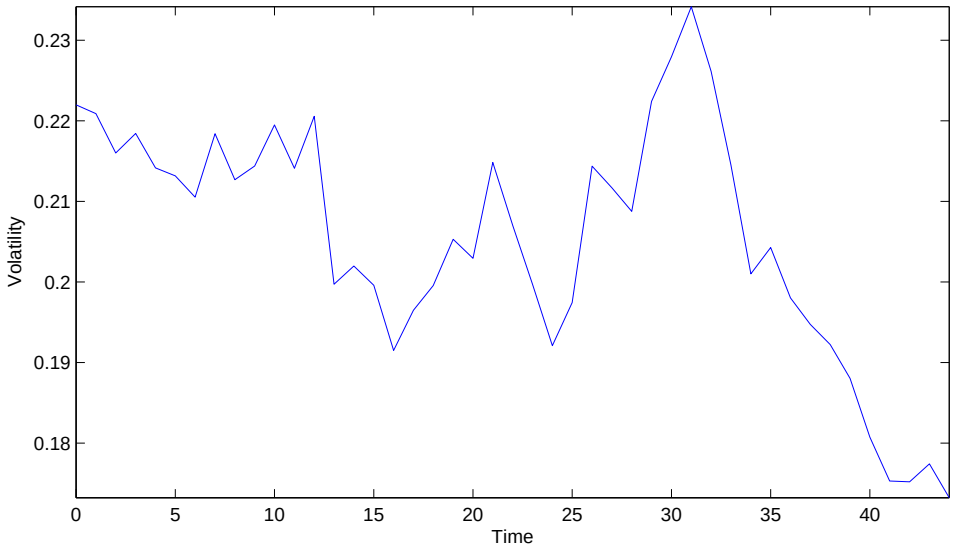

Figure 1.7: This figure displays the daily implied volatility of a 2-month European call option on the Euro Stoxx 50 Index during the period 2010-10-18 to 2010-12-17.

A model with volatility $\sigma(t, S(t))$, where $\sigma(t, S(t))$ is a deterministic function of t and $S(t)$, is commonly referred to as a local volatility model. The Brigo-Mercurio log-normal mixture model that will be presented in this thesis is a local volatility model.

An important special case of local volatility is when $\sigma(t)$ is a deterministic function of $t \in [0, T]$. This case is thoroughly discussed in Section 3.1.

1.4 Volatility Smile

Clearly, for real market data we only have a finite number of implied volatilities (corresponding to a equally many strike prices). But if we interpolate the implied volatility at a fixed time we get smooth curves $K \mapsto \sigma_{imp}(K)$. These curves typically has skewed or smiley shapes meaning that the implied volatility is high for low strikes and low for high strikes or that it has a minimum around the underlying forward price. In connection with options on stocks the smiley phenomenon is commonly identified and it is widely known and recognized as the volatility smile or smiles in the volatility structure.

In Figure 1.8 we can see the implied volatility interpolated from 9 different strikes and corresponding implied volatilities.

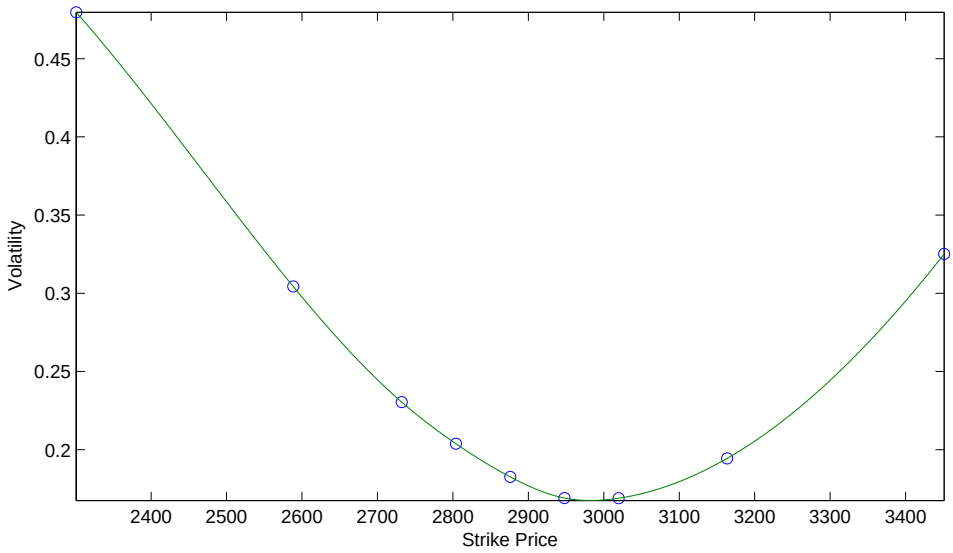

Figure 1.8: An illustration of the volatility smile using market data on 2010-11-05 with 10 days left to maturity.

Often it is interesting to see how this smile evolves with different times to maturity i.e. term structure. We then get a surface which is commonly known as the implied volatility surface. In Figure 1.9 we see the implied volatility surface over a 2-month period.

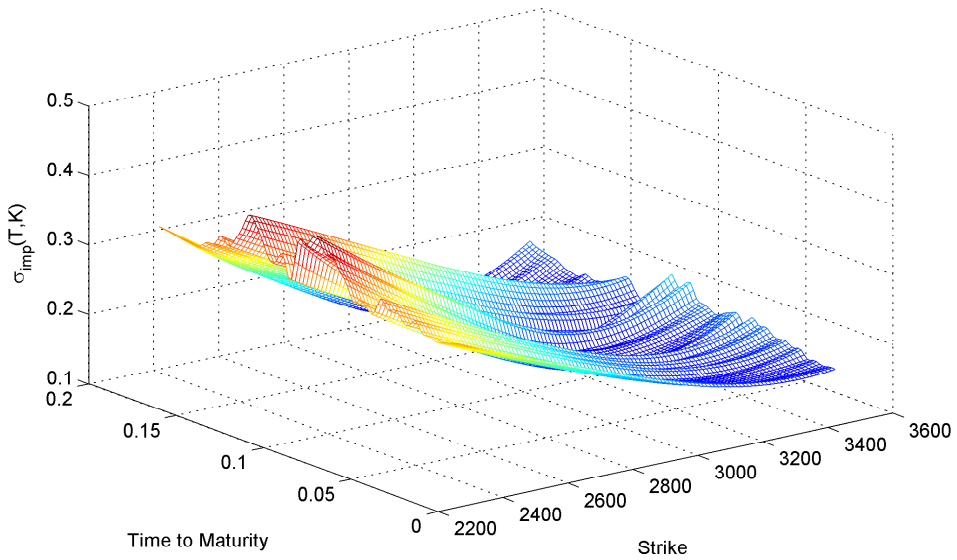

Figure 1.9: This figure displays the implied volatility surface during the period 2010-10-18 to 2010-12-17.

It is clearly a good point if a model can capture the volatility smile property of the market. The Brigo-Mercurio generalization of the Black-Scholes model that will be presented in this thesis leads to smiles in the volatility structure which we illustrate at the end of Section 5.2. Then in Section 5.3 it is proved that the implied volatility has a local minimum at the underlying forward price.

Chapter 2

Implied risk-neutral distribution

In this section we present a way to obtain the risk-neutral marginal distribution of the asset price process $S = (S(t))_{0 \leq t \leq T}$ from the market price of European call options. We will compare the implied density of $S(T)$ with the density of $S(T)$ in the Black-Scholes model i.e. a log-normal density. Finally, we will see that a mixture of log-normals gives a better fit to the implied density compared with only one log-normal density.

The price at time zero of a European call with strike K on S is

$$c(0, x, T, K) = E\left[e^{-rT}(S(T) - K)^+\right],$$

where $x = S(0)$ and E denotes the expectation with respect to the risk-neutral measure. Let $p = p(0, x, T, y)$ be the risk-neutral marginal density of $S(T)$ i.e. p is defined by

$$P(S(T) \in A) = \int_A p(0, x, T, y)dy, \quad \forall A \in \mathcal{B}(\mathbb{R}),$$

where $\mathcal{B}(\mathbb{R})$ denotes the Borel σ-algebra on $\mathbb{R}$. We can then write

$$\begin{aligned} c(0, x, T, K) &= e^{-rT} \int_0^\infty (y - K)^+ p(0, x, T, y)dy \\ &= e^{-rT} \int_K^\infty (y - K)p(0, x, T, y)dy. \end{aligned}$$

Now, if we differentiate twice with respect to K we get

$$p(0, x, T, K) = e^{rT} \frac{\partial^2 c}{\partial K^2}(0, x, T, K). \tag{2.1}$$

Equation (2.1) is often called the Breeden-Litzenberger formula and it provides a way to calculate the risk-neutral distribution of $S(T)$ from European

call option prices. The problem when using this in practice is that it only exists at most a finite number of call prices corresponding to equally many strike prices. The market data used in this thesis has 9 different call prices corresponding to 9 different strike prices. So the numerical differentiation will most likely be a bit rough.

First it is a good idea to create new prices for calls corresponding to new strikes by interpolating over the 9 prices we do have. Then, after interpolation, we must perform numerical differentiation. However, numerical differentiation is an ill-posed problem and it is a balance between stability and precision. Since we are going to differentiate twice it seems as a good idea to interpolate a piecewise cubic curve to the 9 data points. Then the second derivatives will be piecewise affine, but this is more desirable than to interpolate a higher order curve since the estimates of the derivative will then not be as precise compared with the piecewise cubic case. In other words, if we would want to have a smoother second derivative curve we would loose precision.

The result from using equation (2.1) on a 1-month option during Period 2 (described in Section 6.1) can be seen in Figure 2.1.

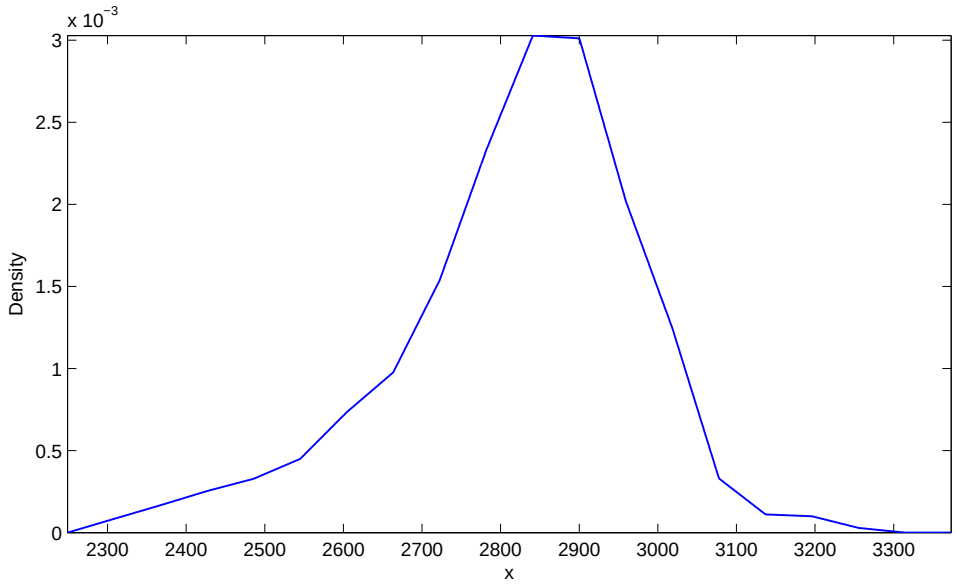

Figure 2.1: This figure displays the implied density of $S(T)$ from equation (2.1) during Period 2.

In Figure 2.2 we compare the implied density of $S(T)$ from Figure 2.1 with the density of $S(T)$ in the Black-Scholes model. Here, remember that that in the Black-Scholes model $S(T)$ is a log-normal random variable. Recall

that the log-normal density function with parameters μ and σ equals

$$f(x;\mu,\sigma) = \frac{1}{x\sigma\sqrt{2\pi}} e^{-\frac{(\ln x-\mu)^2}{2\sigma^2}}, \quad x > 0.$$

Here, we fit the log-normal density function by manually choosing the parameters μ and σ.

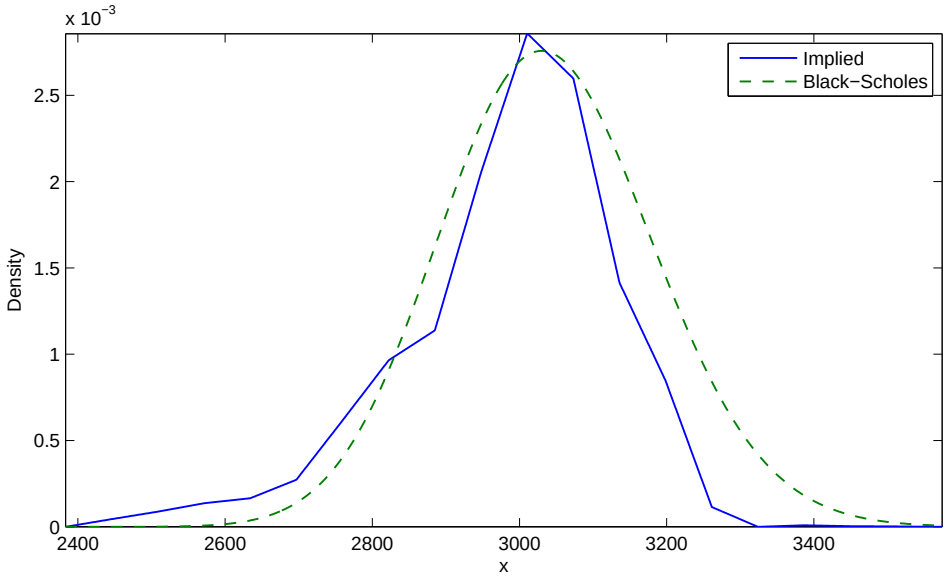

Figure 2.2: Comparison between the implied density of $S(T)$ from equation (2.1) and the density of of $S(T)$ in the Black-Scholes model during Period 2.

The comparison shows that although the log-normal density of $S(T)$ seems to fit the implied density pretty well it is obvious that the log-normal density has a too heavy right tail and a not heavy enough left tail.

A mixture of log-normal densities is simply a convex combination of log-normal densities. The following equation yields a mixture of two log-normal densities:

$$\begin{cases} \lambda_1 f(x;\mu_1,\sigma_1) + \lambda_2 f(x;\mu_2,\sigma_2), \\ \lambda_1 + \lambda_2 = 1, \ \lambda_1 \geq 0, \lambda_2 \geq 0. \end{cases}$$

By mixing two log-normal densities we can achieve a better fit to the implied density of $S(T)$ in the sense that we can get a heavier left tail and a slightly less heavy right tail. The parameters in Table 2.1 are used to demonstrate this in Figure 2.3 where, again, the parameters are manually chosen to get a good fit.

	Black-Scholes	Mixture	
μ	8.0187	7.9487	8.0187
σ	0.0477	0.0583	0.0397
λ	1	0.21	0.79

Table 2.1: The parameters used in Figure 2.3

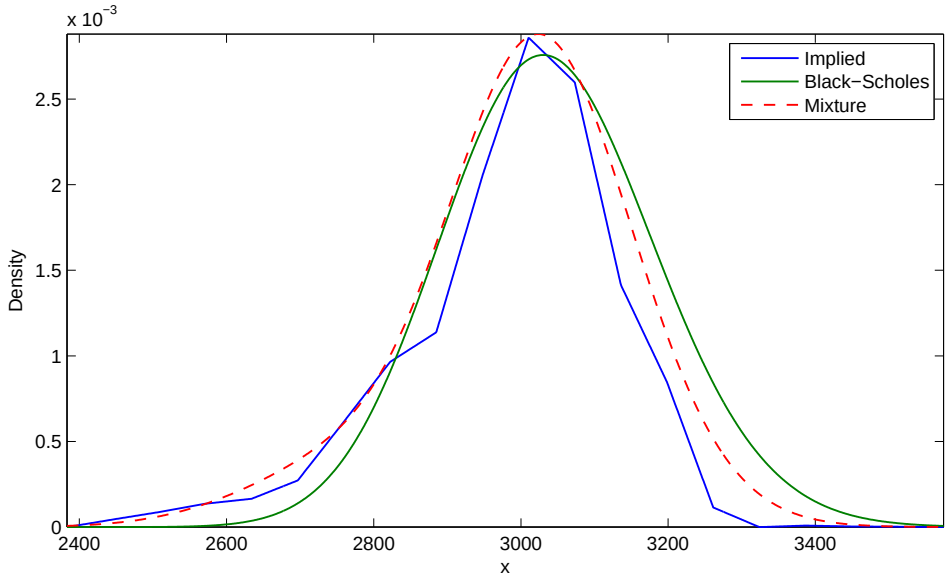

Figure 2.3: Comparison between the implied density of $S(T)$ from equation (2.1), the density of of $S(T)$ in the Black-Scholes model, and a mixture of two log-normal densities during Period 2.

Chapter 3

Delta-Hedging in a local volatility model

In option pricing with local volatility we start with a representation of the stock price process $S = (S(t))_{0 \leq t \leq T}$ such that

$$dS(t) = S(t)(rdt + \sigma(t, S(t))dW(t))$$

where $\sigma : [0, T] \times \mathbb{R}_+ \to \mathbb{R}_+$, $r \in \mathbb{R}_+$, and W is a standard Brownian motion under the risk-neutral probability measure P. Throughout this thesis the set $\mathbb{R}_+$ denotes the set of positive real numbers. Moreover let the bond price process $B = (B(t))_{0 \leq t \leq T}$ be given by

$$dB(t) = rB(t)dt.$$

Under appropriate regularity conditions on $\sigma(t, y)$ it follows that S/B is a martingale under P and therefore P is also called a martingale measure.

Consider a simple European styled derivative paying the amount $f(S(T))$ at time T. Assume $v(t, S(t))$ is the price of this derivative at time t and that v is smooth. Our aim in this section is to prove the existence of a portfolio strategy $h = (h_S, h_B)$ that is self-financing, that is

$$\begin{cases} v(t, S(t)) = h_S(t)S(t) + h_B(t)B(t) \\ dv(t, S(t)) = h_S(t)dS(t) + h_B(t)dB(t). \end{cases}$$

Consider a portfolio which at time t is long one derivative and short Δ shares of the stock. The value of the portfolio at time t is then

$$\Pi(t) = v(t, S(t)) - \Delta S(t).$$

Next, we define the infinitesimal portfolio return $\mathbf{d}\Pi(t)$ (not to be confused with the stochastic differential) by

$$\mathbf{d}\Pi(t) = dv(t, S(t)) - \Delta dS(t)$$

and we want to choose $\Delta = \Delta(t)$ such that the noisy part of $\mathbf{d}\Pi(t)$ disappears. By Itô's lemma we get

$$\mathbf{d}\Pi(t) = \frac{\partial v}{\partial t}(t, S(t))dt + \frac{\partial v}{\partial s}(t, S(t))dS(t) + \frac{1}{2}\frac{\partial^2 v}{\partial s^2}(t, S(t))(dS(t))^2 - \Delta dS(t)$$
$$= \frac{\partial v}{\partial t}(t, S(t))dt + \frac{\partial v}{\partial s}(t, S(t))dS(t) + \frac{\sigma^2(t, S(t))}{2}S^2(t)\frac{\partial^2 v}{\partial s^2}(t, S(t))dt - \Delta dS(t).$$

If we set

$$\Delta = \frac{\partial v}{\partial s}(t, S(t))$$

the noisy part of the portfolio disappears and we get

$$\mathbf{d}\Pi(t) = \frac{\partial v}{\partial t}(t, S(t))dt + \frac{\sigma^2(t, S(t))}{2}S^2(t)\frac{\partial^2 v}{\partial s^2}(t, S(t))dt.$$

Now the portfolio is risk-free and the infinitesimal price increment must be

$$\mathbf{d}\Pi(t) = r\Pi(t)dt = \Pi(t)\frac{dB(t)}{B(t)}$$

and, hence,

$$\frac{\partial v}{\partial t}(t, S(t))dt + \frac{\sigma^2(t, S(t))}{2}S^2(t)\frac{\partial^2 v}{\partial s^2}(t, S(t))dt$$
$$-r\Big(v(t, S(t)) - S(t)\frac{\partial v}{\partial s}(t, S(t))\Big)dt = 0.$$

This equation is satisfied if

$$\begin{cases} \dfrac{\partial v}{\partial t}(t, s)dt + s^2\dfrac{\sigma^2(t, s)}{2}\dfrac{\partial^2 v}{\partial s^2}(t, s)dt - r\Big(v(t, s) - s\dfrac{\partial v}{\partial s}(t, s)\Big)dt = 0, \\ v(T, s) = f(s), 0 \le t < T, s > 0, \end{cases}$$

and the Feynman-Kac connection gives us that

$$v(t, S(t)) = e^{-r(T-t)}E\left[f(S(T))|S(t) = s\right].$$

Now if we define

$$h_S(t) = \frac{\partial v}{\partial s}(t, S(t))$$

and

$$h_B(t) = \frac{v(t, S(t)) - h_S(t)S(t)}{B(t)}$$

it follows that

$$\begin{cases} v(t, S(t)) = h_S(t)S(t) + h_B(t)B(t) \\ dv(t, S(t)) = h_S(t)dS(t) + h_B(t)dB(t). \end{cases}$$

In other words, the portfolio strategy h is self-financing and replicates the derivative.

3.1 An important special case

We now consider the special case when $\sigma(t)$, $0 \leq t \leq T$, is a deterministic positive function and the stock price process $S = (S(t))_{0 \leq t \leq T}$ is governed by the equation

$$dS(t) = S(t)(rdt + \sigma(t)dW(t)). \tag{3.1}$$

This kind of diffusion process is important since it is of the kind we will use to create a mixture dynamics in Chapter 5. This model leads us us to explicit formulas for the marginal density of S as well as the price of a call (or put) option. The marginal density of S is defined by $p(t,y)dy = P(S(t) \in dy)$ or equivalently

$$P(S(t) \in A) = \int_A p(t,y)dy, \quad \forall A \in \mathcal{B}(\mathbb{R}), \ t \in [0,T].$$

By using Itô's lemma to compute $d(\ln S(t))$ we find

$$\begin{aligned} d(\ln S(t)) &= \frac{1}{S(t)}dS(t) - \frac{1}{2S^2(t)}(dS(t))^2 \\ &= \left(r - \frac{\sigma^2(t)}{2}\right)dt + \sigma(t)dW(t) \end{aligned}$$

and accordingly from this

$$S(t) = S(0)\exp\left(\int_0^t \Big(r - \frac{\sigma^2(u)}{2}\Big)du + \int_0^t \sigma(u)dW(u)\right).$$

To simplify notation we introduce

$$V(t) = \sqrt{\int_0^t \sigma^2(u)du}$$

so that

$$\int_0^t \sigma(u)dW(u) = V(t)G \tag{3.2}$$

where $G \in N(0,1)$. We then find that

$$\begin{aligned} P(S(t) \leq y) &= P\left(G \leq \frac{1}{V(t)}\left(\ln\frac{y}{S(0)} - rt + \frac{V^2(t)}{2}\right)\right) \\ &= \Phi\left(\frac{1}{V(t)}\left(\ln\frac{y}{S(0)} - rt + \frac{V^2(t)}{2}\right)\right), \end{aligned}$$

where

$$\Phi(x) = \int_{-\infty}^x \varphi(y)dy$$

and

$$\varphi(x) = \frac{e^{-\frac{x^2}{2}}}{\sqrt{2\pi}},\ x \in \mathbb{R}.$$

Differentiating with respect to y yields

$$\begin{aligned} p(t,y) &= \frac{1}{yV(t)}\varphi\left(\frac{1}{V(t)}\left[\ln\frac{y}{S(0)} - rt + \frac{V^2(t)}{2}\right]\right) \\ &= \frac{1}{yV(t)\sqrt{2\pi}}\exp\left(-\frac{1}{2V^2(t)}\left[\ln\frac{y}{S(0)} - rt + \frac{V^2(t)}{2}\right]^2\right). \end{aligned}$$

If (3.1) holds and r is the interest rate, then it is also straightforward to derive an explicit price formula for the call option with strike K and time of maturity T. The call price at time 0 is

$$\begin{aligned} c(0,S(0),K,T) &= e^{-rT}E\left[(S(T)-K)^+\right] \\ &= e^{-rT}E\Big[\big(se^{\int_0^T\left(r-\frac{\sigma^2(u)}{2}\right)du+\int_0^T\sigma(u)dW(u)} - K\big)^+\Big]\Big|_{s=S(0)}. \end{aligned}$$

Again, to simplify notation we introduce

$$a = \int_0^T \big(r - \frac{\sigma^2(u)}{2}\big)du$$

and recall (3.2). We then get

$$\begin{aligned} &E\Big[\big(se^{\int_0^T\left(r-\frac{\sigma^2(u)}{2}\right)du+\int_0^T\sigma(u)dW(u)} - K\big)^+\Big] = E\Big[\big(se^{a-V(T)G} - K\big)^+\Big] \\ &= \int_{-\infty}^{\infty}\big(se^{a-xV(T)} - K\big)^+ e^{-\frac{x^2}{2}}\frac{dx}{\sqrt{2\pi}} \\ &= \int_{-\infty}^{\frac{1}{V(T)}(\ln\frac{s}{K}+a)}\big(se^{a-xV(T)} - K\big)e^{-\frac{x^2}{2}}\frac{dx}{\sqrt{2\pi}} \\ &= se^{a+\frac{V(T)^2}{2}}\Phi\Big(\frac{1}{V(T)}(\ln\frac{s}{K} + a + V(T)^2)\Big) - K\Phi\Big(\frac{1}{V(T)}(\ln\frac{s}{K}+a)\Big). \end{aligned}$$

Thus

$$c(0,s,K,T) = s\Phi(d_1) - Ke^{-rT}\Phi(d_2)$$

where

$$d_1 = \frac{\ln\frac{s}{K} + \big(r + \frac{V^2(T)}{2T}\big)T}{V(T)}$$

and

$$d_2 = \frac{\ln \frac{s}{K} + \big(r - \frac{V^2(T)}{2T}\big)T}{V(T)}.$$

To emphasize the dependence on V we will sometimes write

$$c(0, s, K, T) = c\Big(0, s, K, T; \frac{V(T)}{\sqrt{T}}\Big).$$

Chapter 4

Numerical solution of a PDE

To compute call option prices in the local volatility model that will be presented in Chapter 5 we are led to a parabolic differential equation of the following type

$$\begin{cases} \dfrac{\partial u}{\partial t} + rx\dfrac{\partial u}{\partial x} + \dfrac{1}{2}x^2\sigma^2(t,x)\dfrac{\partial^2 u}{\partial x^2} - ru = 0, & (t,x) \in [0,T[\times \mathbb{R}_+, \\ u(T,x) = (x-K)^+, & x \in \mathbb{R}_+, \end{cases} \tag{4.1}$$

where $\sigma(t,x)$ is a local volatility function such that $0 < \sigma_m < \sigma(t,x) < \sigma_M < \infty$.

In order to solve this equation we will use the implicit (i.e. forward) Euler finite difference method. First we must bound the domain of x into a compact interval $[a,b]$ and impose suitable boundary conditions at $x = a$ and $x = b$. We simply choose the Black-Scholes call prices as boundary conditions. More precisely, if $c_{BS}(t,x,K,T;\sigma)$ denotes the Black-Scholes call price, at time t, of a call option with strike K, time of maturity T, and volatility σ we set

$$\begin{cases} u(t,a) = c_{BS}(t,a,K,T;\sigma(t,a)), & t \in [0,T], \\ u(t,b) = c_{BS}(t,b,K,T;\sigma(t,b)), & t \in [0,T]. \end{cases}$$

Next we introduce a grid of mesh points $(t,x) = (t_n, x_j)$ where $x_j = a + jh$ and $t_n = nk$, $j \in \{0,1,...,J\}$ and $n \in \{0,1,...,N\}$. Here h is the mesh-width in x, k is the time step, $x_J = b$ and $t_N = T$.

Then introduce the forward and backward difference quotients with respect to x

$$\partial_x U_j^n = \frac{U_{j+1}^n - U_j^n}{h}$$
$$\bar{\partial}_x U_j^n = \frac{U_j^n - U_{j-1}^n}{h}$$

and the forward difference quotients with respect to t

$$\partial_t U_j^n = \frac{U_j^{n+1} - U_j^n}{k}$$

In order to approximate the first derivative of u with respect to x we use a central difference quotient

$$\frac{\partial_x U_j^n + \bar{\partial}_x U_j^n}{2h} = \frac{U_{j+1}^n - U_{j-1}^n}{2h}$$

and the second order derivative of u with respect to x is approximated by

$$\partial_x \bar{\partial}_x U_j^n = \partial_x \frac{U_j^n - U_{j-1}^n}{h} = \frac{U_{j-1}^n - 2U_j^n + U_{j+1}^n}{h^2}.$$

The discretizised partial differential equation now becomes

$$\frac{U_j^{n+1} - U_j^n}{k} + rx_j \frac{U_{j+1}^n - U_{j-1}^n}{2h} + \frac{1}{2} x_j^2 \sigma_{n,j}^2 \frac{U_{j-1}^n - 2U_j^n + U_{j+1}^n}{h^2} - rU_j^n = 0$$

for $j = 1, ..., J-1$ and $n = 1, ..., N-1$ where $\sigma_{n,j} = \sigma(t_n, x_j)$. We can rewrite these equations as

$$U_j^{n+1} = a_{n,j} U_{j-1}^n + b_{n,j} U_j^n + c_{n,j} U_{j+1}^n$$

for $j = 1, ..., J-1$ and $n = 1, ..., N-1$, where

$$\begin{aligned} a_{n,j} &= -\left(\frac{k x_j^2 \sigma_{n,j}^2}{2h^2} - \frac{k r x_j}{2h} \right), \\ b_{n,j} &= 1 + rk + \frac{k x_j^2 \sigma_{n,j}^2}{h^2}, \\ c_{n,j} &= -\left(\frac{k x_j^2 \sigma_{n,j}^2}{2h^2} + \frac{k r x_j}{2h} \right). \end{aligned}$$

Noting that U_0^n and U_J^n are given boundary conditions we get

$$\begin{bmatrix} b_{n,1} & c_{n,1} & 0 & \dots & 0 \\ a_{n,2} & b_{n,2} & c_{n,2} & \dots & 0 \\ \vdots & \ddots & \ddots & \ddots & \vdots \\ \vdots & & \ddots & \ddots & c_{n,J-2} \\ 0 & \dots & 0 & a_{n,J-1} & b_{n,J-1} \end{bmatrix} \begin{bmatrix} U_1^n \\ U_2^n \\ \vdots \\ \vdots \\ U_{J-1}^n \end{bmatrix} = \begin{bmatrix} U_1^{n+1} \\ U_2^{n+1} \\ \vdots \\ \vdots \\ U_{J-1}^{n+1} \end{bmatrix} - \begin{bmatrix} a_{n,1} U_0^n \\ 0 \\ \vdots \\ 0 \\ c_{n,J-1} U_J^n \end{bmatrix} \tag{4.2}$$

for $n = N-1, ..., 1, 0$. To solve these equations we use the very efficient tridiagonal matrix algorithm [4] also known as Thomas algorithm[1]. We demonstrate the algorithm with a less heavy notation

$$\begin{bmatrix} b_1 & c_1 & 0 & \dots & 0 \\ a_2 & b_2 & c_2 & \dots & 0 \\ \vdots & \ddots & \ddots & \ddots & \vdots \\ \vdots & & \ddots & \ddots & c_{J-2} \\ 0 & \dots & 0 & a_{J-1} & b_{J-1} \end{bmatrix} \begin{bmatrix} x_1 \\ x_2 \\ \vdots \\ \vdots \\ x_{J-1} \end{bmatrix} = \begin{bmatrix} d_1 \\ d_2 \\ \vdots \\ \vdots \\ d_{J-1} \end{bmatrix} \tag{4.3}$$

or equivalently, the equations

$$\begin{cases} b_1 x_1 + c_1 x_2 = d_1 & \text{if } i = 1, \\ a_i x_{i-1} + b_i x_i + c_i x_{i+1} = d_i & \text{if } i = 2, 3, ..., J-1, \\ a_{J-1} x_{J-2} + b_{J-1} x_{J-1} = d_{J-1} & \text{if } i = J-1. \end{cases}$$

First we assume that the algorithm is possible to carry out and present the steps of the algorithm. Afterwards we present sufficient conditions for the algorithm to be able to be carried out.

The algorithm consists of two steps. We begin by performing simple Gauss elimination to get an upper triangular matrix and after that we do back substitution. First multiply the first equation by a_2/b_1 and subtract it from the second equation ($i = 2$). The second equation then becomes

$$\big(b_2 - \frac{c_1}{b_1} a_2\big) x_2 + c_2 x_3 = d_2 - \frac{d_1}{b_1} a_2.$$

We define $c_1' = c_1/b_1$ and $d_1' = d_1/b_1$ so that we get the new second equation

$$\big(b_2 - c_1' a_2\big) x_2 + c_2 x_3 = d_2 - d_1' a_2.$$

Note that we have eliminated x_1 from the second equation. Next we eliminate x_2 from the third equation ($i = 3$) by multiplying the new second equation by $a_3/(b_2 - c_1' a_2)$ and subtracting it from the third equation. The third equation then becomes

$$\big(b_3 - \frac{c_2}{b_2 - c_1' a_2} a_3\big) x_3 + c_3 x_4 = d_3 - \frac{d_2 - d_1' a_2}{b_2 - c_1' a_2} a_3.$$

Now we define $c_2' = c_2/(b_2 - c_1' a_2)$ and $d_2' = (d_2 - d_1' a_2)/(b_2 - c_1' a_2)$ and we get the new third equation

$$\big(b_3 - c_2' a_3\big) x_3 + c_3 x_4 = d_3 - d_2' a_3.$$

[1] Named after the British physicist and applied mathematician Llewellyn Thomas. The name 'Thomas algorithm' was given by the American mathematician and computer scientist David Young. See NA Digest Monday, March 4, 1996 Volume 96 : Issue 09
`http://www.netlib.org/na-digest-html/96/v96n09.html`

We can continue in this way and in the last step we eliminate x_{J-2} from the last row. But the coefficients will get increasingly complicated with each new elimination. We can however, inspired by the above, write a recursive scheme for the new coefficients

$$\begin{cases} c'_1 = \dfrac{c_1}{b_1}, \qquad c'_i = \dfrac{c_i}{b_i - c'_{i-1}a_i}, \quad i = 2, ..., J-2, \\ \\ d'_1 = \dfrac{d_1}{b_1}, \qquad d'_i = \dfrac{d_i - d'_{i-1}a_i}{b_i - c'_{i-1}a_i}, \quad i = 2, ..., J-1. \end{cases}$$

With these coefficients we get an upper triangular matrix and can solve the system by performing back substitution

$$\begin{cases} x_{J-1} = d'_{J-1}, \\ x_i = d'_i - c'_i x_{i+1}, \quad i = J-2, ..., 1. \end{cases}$$

However, one must be careful when applying this algorithm. For example, it is important that $b_i - c'_{i-1}a_i \neq 0$, $i = 2, ..., J-1$, and $b_1 \neq 0$. Young proves in [4] that the following conditions are sufficient to to be able to perform this algorithm, namely

$$\begin{cases} b_i > 0, \quad i = 1, ..., J-1, & (4.4) \\ b_1 > |c_1|, & (4.5) \\ b_i \geq |c_i| + |a_i| \quad \text{and} \quad a_i \neq 0, \quad c_i \neq 0, \quad i = 1, ..., J-2, & (4.6) \\ b_{J-1} \geq |a_{J-1}|. & (4.7) \end{cases}$$

Indeed, it is sufficient to show that $b_i - c'_{i-1}a_i > 0$, $i = 2, ..., J-1$, under the conditions (4.4)–(4.7). First we prove that $|c'_i| < 1$, $i = 1, ..., J-2$. It's readily seen using (4.5) that $|c'_1| < 1$. Next, assume that $|c'_i| < 1$ for some $i = 2, ..., J-3$. If it is possible to prove $|c'_{i+1}| < 1$ then by induction we have proven that $|c'_i| < 1$, $i = 1, ..., J-2$. In order to prove $|c'_{i+1}| < 1$ it is sufficient to prove $|b_{i+1} - c'_i a_{i+1}| > |c_{i+1}|$. By using the induction assumption and (4.6) we see that

$$|b_{i+1} - c'_i a_{i+1}| \geq b_{i+1} - c'_i a_{i+1} \geq b_{i+1} - |c'_i a_{i+1}| > b_{i+1} - |a_{i+1}| \geq |c_{i+1}|.$$

This concludes the proof that $|c'_i| < 1$, $i = 1, ..., J-2$. From (4.6) it follows that $b_i > |a_i|$, $i = 2, ..., J-2$, and hence,

$$b_i - c'_{i-1}a_i \geq b_i - |c'_{i-1}a_i| > b_i - |a_i| > 0 \quad i = 2, ..., J-2.$$

Lastly, from (4.4) we get that

$$b_{J-1} - c'_{J-2}a_{J-1} > 0 \quad \text{if} \quad a_{J-1} = 0$$

and otherwise, using (4.7),

$$b_{J-1} - c'_{J-2}a_{J-1} \geq b_{J-1} - |c'_{J-2}a_{J-1}| > b_{J-1} - |a_{J-1}| \geq 0 \quad \text{if} \quad a_{J-1} \neq 0.$$

This concludes the proof that (4.4)–(4.7) are sufficient conditions for being able to carry out the algorithm.

Now we know how to solve a tridiagonal matrix equation in an efficient way and we denote by $(d_{n,1}, ..., d_{n,J-1})$, $n = 1, ..., N-1$ the right hand side of the equations in (4.2). The process for solving our original equations (4.2) then becomes

$$\begin{cases} c'_{n,1} = \dfrac{c_{n,1}}{b_{n,1}}, \quad c'_{n,i} = \dfrac{c_{n,i}}{b_{n,i} - c'_{n,i-1}a_{n,i}}, \quad i = 2, ..., J-2, \\ \\ d'_{n,1} = \dfrac{d_{n,1}}{b_{n,1}}, \quad d'_{n,i} = \dfrac{d_{n,i} - d'_{n,i-1}a_{n,i}}{b_{n,i} - c'_{n,i-1}a_{n,i}}, \quad i = 2, ..., J-1, \\ \\ U^n_{J-1} = d'_{n,J-1}, \quad U^n_i = d'_{n,i} - c'_{n,i}U^n_{i+1}, \quad i = J-2, ..., 1, \end{cases}$$

for each $n = N-1, ..., 1, 0$. When implementing this algorithm in Matlab we check the sufficient conditions (4.4)–(4.7) and terminate the algorithm if the conditions are not satisfied. It is also important to make sure that the quantities $b_{n,i} - c'_{n,i-1}a_{n,i}$ are not too small since then a serious source of round-off errors may arise.

It is interesting to see how much more efficient the Tridiagonal matrix algorithm (TDMA) is compared to using Matlab's function `mldivide` (\) or LU-decomposition on the equations in (4.2). The time consumption is heavily affected by how fine the grid of mesh points is.

For this demonstration we compute the price of a European call option from equation (4.1) using the local volatility function $\sigma(t, x)$ from equation (5.8) in Chapter 5.2 with $S(0) = 2500$, $K = 2500$, $N = 3$, $\varepsilon = 1/252$, $\delta = 2/252$, $\bar{\sigma} = 0.3$, $(\bar{\sigma}_1, \bar{\sigma}_2, \bar{\sigma}_3) = (0.2, 0.3, 0.4)$, $(\lambda_1, \lambda_2, \lambda_3) = (1/3, 1/3, 1/3)$. Moreover, γ_i, $i = 1, 2, 3$ are the affine functions

$$\gamma_i(t) = \bar{\sigma} + (t - \varepsilon)\frac{\bar{\sigma}_i - \bar{\sigma}}{\delta - \varepsilon}, \quad t \in [\varepsilon, \delta], i = 1, 2, 3.$$

We choose the grid of mesh points:

$$\begin{cases} x_j = 1000 + j, \quad j = 0, ..., 1999, \\ t_n = \dfrac{n}{5 \cdot 252}, \quad n = 0, ..., 220. \end{cases}$$

i.e. $h = 1$ and $k = 1/(5 \cdot 252)$. These parameters will be used throughout this Chapter if not stated otherwise. Considering (4.2), we must now solve 220

	TDMA	\	LU
Time	0.09s	12.12s	21.04s

Table 4.1: Time consumption for solving (4.2) for $n = 219, 218, ..., 0$.

matrix equations of the dimension 1999×1999. The time consumption, based on solving (4.1) once with the above parameters, is presented in Table 4.1

Even more interesting is to see how accurate this PDE solution is by comparing it with the solution obtained by Monte Carlo simulation. For the Monte Carlo simulation we use the Euler-Maruyama method with 10^6 simulations. For the first comparison we let $K = 2500$ and $S(0) = 2500$ and the result can be seen in the following table:

Time	PDE	MC
t_{20}	90.79	90.97
t_{30}	68.74	68.78

If $K = 2200$ and $S(0) = 2500$ we get the following result:

Time	PDE	MC
t_{20}	310.47	310.46
t_{30}	28.59	28.76

With these results we are now more confident that the PDE solution is accurate enough.

An alternative approach to solving (4.1) is to first simplify the equation by making the substitutions

$$\begin{cases} x = e^y \\ v(t, y) = u(t, x) \end{cases}$$

so that the PDE (4.1) transforms into

$$\begin{cases} \dfrac{\partial v}{\partial t} + \Big(r - \dfrac{1}{2}\sigma^2(t, e^y)\Big)\dfrac{\partial v}{\partial y} + \dfrac{1}{2}\sigma^2(t, e^y)\dfrac{\partial^2 v}{\partial y^2} - rv = 0, \quad (t, y) \in [0, T[\times\mathbb{R} \\ v(T, y) = (e^y - K)^+, \quad y \in \mathbb{R}. \end{cases} \tag{4.8}$$

This should give increased stability when solving it numerically. If $0 < \sigma_m < \sigma(t, e^y) < \sigma_M < \infty$ we solve this equation using the implicit Euler finite difference method in exactly the same fashion as above. We get the

coefficients:

$$a_{n,j} = -\left(\frac{k\sigma_{n,j}^2}{2h^2} - \frac{kr - \frac{k}{2}\sigma_{n,j}^2}{2h}\right),$$
$$b_{n,j} = 1 + rk + \frac{k\sigma_{n,j}^2}{h^2},$$
$$c_{n,j} = -\left(\frac{k\sigma_{n,j}^2}{2h^2} + \frac{kr - \frac{k}{2}\sigma_{n,j}^2}{2h}\right),$$

for $j = 1, ..., J-1$ and $n = 1, ..., N-1$.

We denote by PDE 1 and PDE 2 the solutions from the previous and the new transformed equations respectively. It is interesting to see if there is any difference in the accuracy of the two solutions. To this end we use the same data and parameters as above with $K = S(0) = 2500$ and we get the following result:

Time	PDE 1	PDE 2	MC
t_{20}	90.79	90.79	90.97
t_{30}	68.74	68.74	68.78

If $K = 2200$ and $S(0) = 2500$ we get:

Time	PDE 1	PDE 2	MC
t_{20}	310.47	310.47	310.46
t_{30}	303.52	303.52	303.41

These results indicates that there is no significant difference in accuracy between the two PDE solutions. Furthermore, the two solutions are both extremely fast when using the TDMA-algorithm. The times in Table 4.2 are based on solving the two PDEs once for each of the method three methods.

In order to test whether one of the two PDEs is faster to solve than the other, with the parameters defined as above, we will solve the each PDE 1000 times and calculate the average times. We do this only for the TDMA-algorithm and the results are presented in Table 4.2. We can conclude that with the parameters defined as above there is hardly no difference in computational speed between the two PDEs.

	TDMA	\	LU
Time (PDE 1)	0.09s	12.12s	21.04s
Time (PDE 2)	0.07s	12.01s	22.04s

Table 4.2: Time consumption for solving (4.2) for $n = 219, 218, ..., 0$.

	TDMA
Time (PDE 1)	0.0875s
Time (PDE 2)	0.0873s

Table 4.3: Average time consumption for solving (4.2) for $n = 219, 218, ..., 0$.

Finally we examine the rate of convergence when making the grid of mesh points increasingly fine. Using the same parameters as previously in this chapter with $K = S(0) = 2500$ we decrease the step size h, starting at $h = 100$. In this particular case they seem to converge equally fast, which can be seen in Figure 4.1.

There seems to be no obvious advantages using the transformed equation (4.8) over (4.1) when applying the Implicit Euler method.

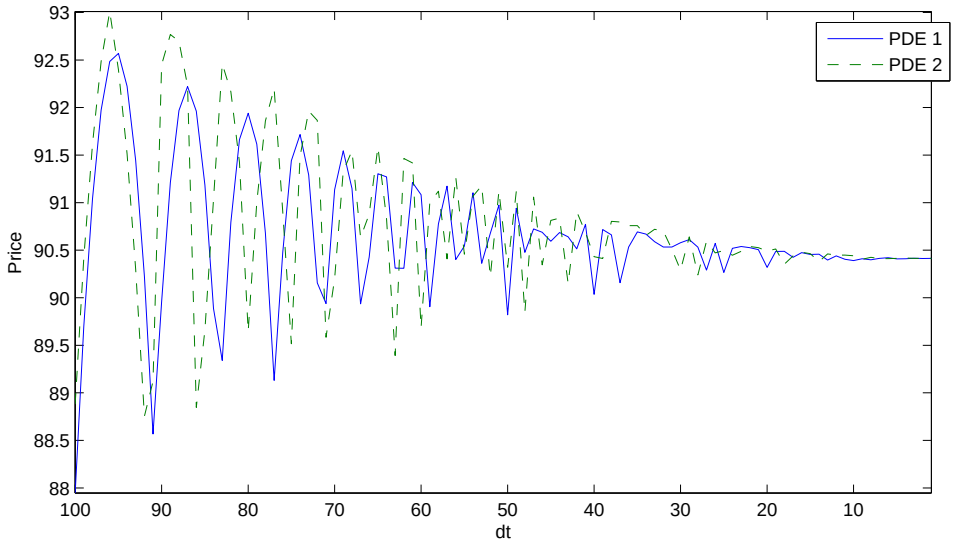

Figure 4.1: Rate of convergence for the two PDE-solutions, in a particular case, as h decreases.

Chapter 5

A mixture dynamics model

5.1 Background

In discrete time, mixture models in connection to option pricing have been studied early on by Ritchey [5] and subsequently by Melick and Thomas [6], and Guo [7].

Possibly inspired by these papers, Brigo and Mercurio [1] developed a continuous time diffusion model in option pricing. In particular, they proved, under the risk-neutral measure, that if the local volatility function is chosen in a particular way the density of the asset price process at any fixed time will be a convex combination of densities from known given distributions. A special case of this is the mixture of log-normal densities that we investigate in this thesis.

This approach leads to a model that is complete and has smiles in the volatility structure.

5.2 Mixture of log-normals

In this section we briefly present the mathematical theory behind the mixture dynamics model by Brigo and Mercurio in a special case. We begin by defining N diffusion processes $S_i = (S_i(t))_{t\geq 0}$, $i = 1, ..., N$, which we will always think of as given. Then we use these N diffusion processes in order to define the dynamics of the asset price process $S = (S(t))_{t\geq 0}$.

Under a certain probability measure P we consider the diffusion processes

$$\begin{cases} dS_i(t) = rS_i(t)dt + \sigma_i(t)S_i(t)dW(t), \quad i = 1, ..., N, \quad 0 < t \leq T \\ S_i(0) = S_0, \end{cases} \tag{5.1}$$

where $r \geq 0$ and

$$\sigma_i(t) = \begin{cases} \bar{\sigma}, & t \in [0, \varepsilon] \\ \gamma_i(t), & t \in (\varepsilon, \delta] \\ \bar{\sigma}_i, & t \in (\delta, T] \end{cases} \tag{5.2}$$

where $\bar{\sigma}, \bar{\sigma}_i \in \mathbb{R}_+$ and $\gamma_i : (\varepsilon, \delta] \longrightarrow \mathbb{R}_+$ is any smooth function such that $\sigma_i(t)$ is continuous, $i = 1, ..., N$. The reason why we assume all $\sigma_i(t)$, $i = 1, ..., N$ to be equal for every $t \in [0, \varepsilon]$ will be explained later when we have an explicit expression for $\sigma(t, y)$. In Figure 5.1 we can see an example of how $\sigma_i(t)$ looks like if $\varepsilon = 1$, $\delta = 2$, $T = 5$, $\bar{\sigma} = 0.25$, $\bar{\sigma}_i = 0.20$ and γ_i is an affine function.

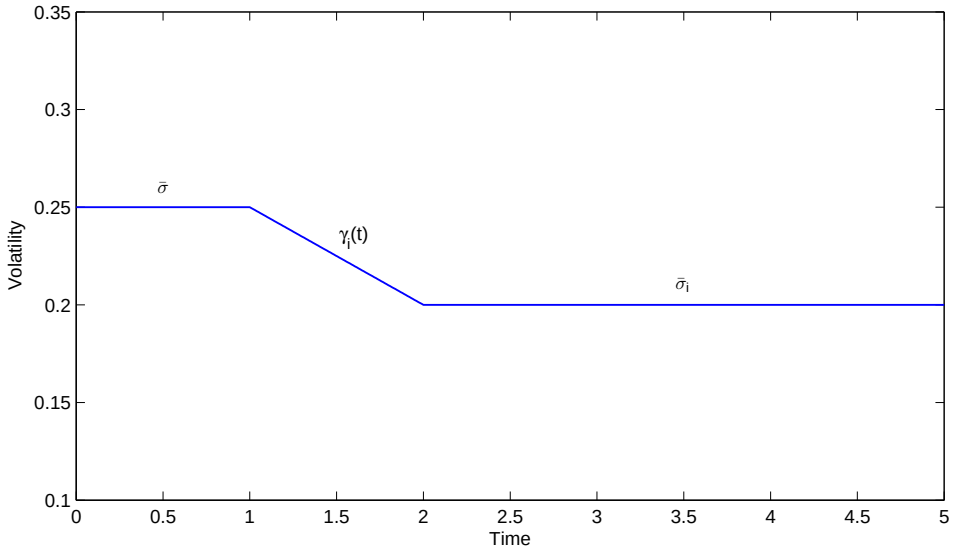

Figure 5.1: An example of how $\sigma_i(t)$ can look like if $\varepsilon = 1$, $\delta = 2$, $T = 5$, $\sigma_0 = 0.25$, $\sigma_i = 0.20$ and γ_i is an affine function.

For fixed $i \in \{1, ..., N\}$ let $p_i(t, \cdot)$ be the density of $S_i(t)$, defined by

$$P(S_i(t) \in A) = \int_A p_i(t, y) dy.$$

In Chapter 3.1 we derived an explicit expression for $p_i(t, y)$, viz.

$$p_i(t, y) = \frac{1}{y V_i(t) \sqrt{2\pi}} \exp\left(-\frac{1}{2V_i^2(t)} \left[\ln \frac{y}{S_0} - rt + \frac{V_i^2(t)}{2} \right]^2 \right) \tag{5.3}$$

where

$$V_i(t) = \sqrt{\int_0^t \sigma_i^2(s) ds}.$$

Now we try to define the dynamics of the asset price process $S = (S(t))_{t\geq 0}$ by

$$\begin{cases} dS(t) = rS(t)dt + \sigma(t, S(t))S(t)dW(t) \\ S(0) = S_0 \end{cases} \tag{5.4}$$

where $\sigma : [0, T] \times \mathbb{R}_+ \to \mathbb{R}_+$ is a continuous function such that

$$p(t, y) = \sum_{i=1}^{N} \lambda_i p_i(t, y) \tag{5.5}$$

and where $\lambda_i \in [0, 1]$, $i = 1, ..., N$, $\lambda_1 + ... + \lambda_N = 1$, and $p(t, \cdot)$ is the density of $S(t)$ for each $0 < t \leq T$.

Note that since

$$P[S_0 \leq x] = \begin{cases} 1, & x \geq S_0 \\ 0, & x < S_0 \end{cases}$$

we have have $p(0, \cdot) = p_i(0, \cdot) = \delta_{S_0}(\cdot)$ where δ_a is the Dirac delta probability measure centered at a.

Next we will utilize the Kolmogorov forward equation in order to retrieve the diffusion equation (5.4) from the density p and in that way determine what $\sigma(t, y)$ must be. The following theorem holds under some technical assumptions (see [8] for details).

Theorem 1. (Kolmogorov Forward Equation)
Let $s < t$ and define the transition probability density

$$p(s, x; t, y)dy = dP(S(t) \in dy | S(s) = x).$$

Then p satisfies the partial differential equation

$$\begin{cases} \dfrac{\partial}{\partial t} p(s, x; t, y) - \dfrac{1}{2} \dfrac{\partial^2}{\partial y^2} (\sigma^2(t, y) y^2 p(s, x; t, y)) + \dfrac{\partial}{\partial y} (ryp(s, x; t, y)) = 0, \\ \lim\limits_{t \to s} p(s, x; t, y)dy = \delta_x(dy). \end{cases}$$

We can use Theorem 1 with $s = 0$ and $x = S_0$ to find $\sigma(t, y)$. We do that by solving the forward Kolmogorov equation

$$\frac{\partial}{\partial t} p(t, y) - \frac{1}{2} \frac{\partial^2}{\partial y^2} (\sigma^2(t, y) y^2 p(t, y)) + \frac{\partial}{\partial y} (ryp(t, y)) = 0 \tag{5.6}$$

given that each p_i satisfies the forward Kolmogorov equation

$$\frac{\partial}{\partial t} p_i(t, y) - \frac{1}{2} \frac{\partial^2}{\partial y^2} (y^2 \sigma_i^2(t) p_i(t, y)) + \frac{\partial}{\partial y} (ryp_i(t, y)) = 0. \tag{5.7}$$

Using (5.5) and the fact that the derivative operator is linear we can rewrite (5.6) in the following way

$$\sum_{i=1}^{N} \lambda_i \frac{\partial}{\partial t} p_i(t,y) - \sum_{i=1}^{N} \lambda_i \frac{1}{2} \frac{\partial^2}{\partial y^2} (\sigma^2(t,y) y^2 p_i(t,y)) + \sum_{i=1}^{N} \lambda_i \frac{\partial}{\partial y} (ry p_i(t,y)) = 0.$$

Then if we use (5.7) and substitute we get

$$\sum_{i=1}^{N} \lambda_i \frac{1}{2} \frac{\partial^2}{\partial y^2} (y^2 \sigma_i^2(t) p_i(t,y)) = \sum_{i=1}^{N} \lambda_i \frac{1}{2} \frac{\partial^2}{\partial y^2} (\sigma^2(t,y) y^2 p_i(t,y)).$$

And again, if we use the linearity of the derivative operator

$$\frac{\partial^2}{\partial y^2} \left[\sum_{i=1}^{N} \lambda_i y^2 \sigma_i^2(t) p_i(t,y) \right] = \frac{\partial^2}{\partial y^2} \left[\sigma^2(t,y) \sum_{i=1}^{N} \lambda_i y^2 p_i(t,y) \right]$$

Integrating both sides twice with respect to y, we get

$$\sigma^2(t,y) \sum_{i=1}^{N} \lambda_i y^2 p_i(t,y) = \sum_{i=1}^{N} \lambda_i y^2 \sigma_i^2(t) p_i(t,y) + yA(t) + B(t)$$

Now we note that the left hand side of this equation must tend to 0 as $y \to \infty$ since

$$\lim_{y \to \infty} y^2 p_i(t,y) = 0$$

and $\sigma(t,y)$ is uniformly bounded for large y. But if the left hand side of the equation tends to zero as $y \to \infty$ then the right hand side must also tend to zero as $y \to \infty$. This can only happen if $A = B = 0$.

This means that when $(t,y) > (0,0)$ we have the following expression for $\sigma(t,y)$, namely

$$\sigma(t,y) = \sqrt{\frac{\sum_{i=1}^{N} \lambda_i \sigma_i^2(t) p_i(t,y)}{\sum_{i=1}^{N} \lambda_i p_i(t,y)}}$$

or, more explicitly

$$\sigma(t,y) = \sqrt{\frac{\sum_{i=1}^{N} \lambda_i \sigma_i^2(t) \frac{1}{V_i(t)} \exp\left\{ -\frac{1}{2V_i^2(t)} \left[\ln \frac{y}{S_0} - rt + \frac{1}{2} V_i^2(t) \right]^2 \right\}}{\sum_{i=1}^{N} \lambda_i \frac{1}{V_i(t)} \exp\left\{ -\frac{1}{2V_i^2(t)} \left[\ln \frac{y}{S_0} - rt + \frac{1}{2} V_i^2(t) \right]^2 \right\}}} \tag{5.8}$$

where

$$V_i(t) = \sqrt{\int_0^t \sigma_i^2(s) ds}, \quad i = 1, ..., N.$$

There are possible problems for a regular behaviour of $\sigma(t,y)$ and as in [1] we let $\sigma_i(t) = \bar{\sigma}$ for every $t \in [0,\varepsilon]$, $i = 1,...,N$ so that

$$\sigma(t,\cdot)\Big|_{[0,\varepsilon]} = \bar{\sigma}.$$

This motivates the choice of $\sigma_i(t)$, $i = 1,...,N$ in (5.2).

In Figure 5.2 we have plotted a realization of $\sigma(t,S(t))$. The stock prices was simulated by using the Euler-Maruyama method on the SDE (5.4) and we let $S_0 = 2500$, $N = 3$, $\varepsilon = 1/252$, $\delta = 2/252$, $\bar{\sigma} = 0.3$, $(\bar{\sigma}_1, \bar{\sigma}_2, \bar{\sigma}_3) = (0.2, 0.3, 0.4)$, $(\lambda_1, \lambda_2, \lambda_3) = (1/3, 1/3, 1/3)$. Moreover, γ_i, $i = 1,2,3$ are the affine functions

$$\gamma_i(t) = \bar{\sigma} + (t-\varepsilon)\frac{\bar{\sigma}_i - \bar{\sigma}}{\delta - \varepsilon}, \quad t \in [\varepsilon, \delta], i = 1,2,3.$$

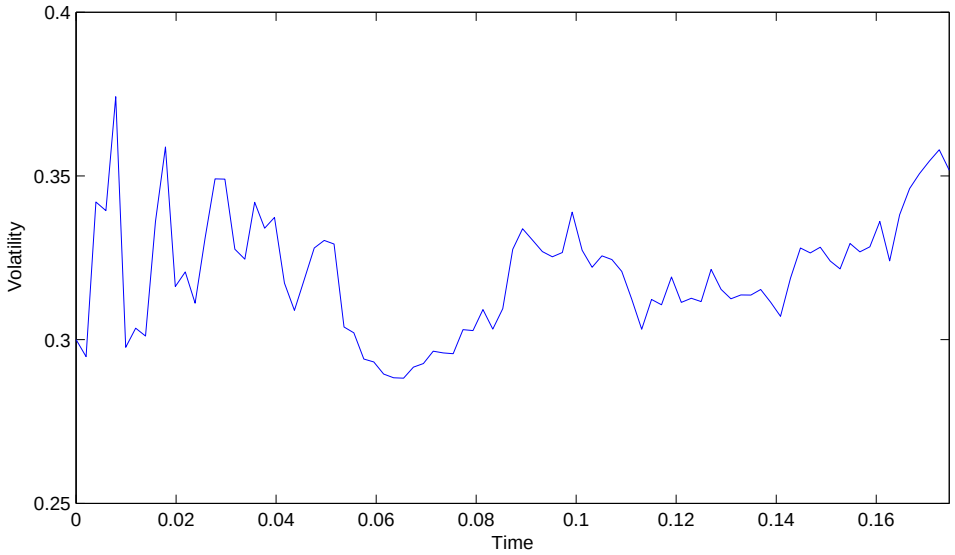

Figure 5.2: A realization of $\sigma(t,S(t))$.

If we set

$$\Lambda_i(t,y) = \frac{\lambda_i p_i(t,y)}{\sum_{i=1}^N \lambda_i p_i(t,y)}, \quad i = 1,...,N \tag{5.9}$$

we get

$$\sigma^2(t,y) = \sum_{i=1}^N \Lambda_i(t,y)\sigma_i^2(t) \tag{5.10}$$

where $\Lambda_i \in [0,1]$, $i = 1,...,N$ are such that $\Lambda_1 + ... + \Lambda_N = 1$. In other words, the squared volatility function is a convex combination of the squared given

volatility functions. From (5.10) we get that $\sigma(t,y)$ is bounded away from zero by a constant σ_m and bounded from above by a constant σ_M where

$$\sigma_m = \inf_{t\geq 0} \min_{i=1,\ldots,N} \sigma_i(t)$$
$$\sigma_M = \inf_{t\geq 0} \max_{i=1,\ldots,N} \sigma_i(t).$$

With $\sigma(t,y)$ defined by (5.8) it is readily seen that the SDE (5.4) has a solution. In fact, if

$$S(t) = S_0 e^{Z(t)}$$

we get

$$dZ(t) = \left(r - \frac{1}{2}\sigma(t,e^{Z(t)})\right)dt + \sigma(t,e^{Z(t)})dW(t)$$

which has a solution and therefore the SDE (5.4) has a solution (for details, see [1]).

We convince ourselves, by numerical investigations, that the basic equation (5.5) actually holds. In other words, we want to numerically check that the relation

$$P(S(T)\in A) = \sum_{i=1}^{N} \lambda_i \int_A p_i(T,y)dy \tag{5.11}$$

holds for some different values of T. In order to estimate the left hand side we utilize the Feynman-Kac connection and solve the partial differential equation

$$\begin{cases} \dfrac{\partial u}{\partial t} + rx\dfrac{\partial u}{\partial x} + \dfrac{1}{2}x^2\sigma^2(t,x)\dfrac{\partial^2 u}{\partial x^2} - ru = 0, \quad (t,x)\in [0,T[\times\mathbb{R}_+, \\ u(T,x) = 1_A(x), \quad x\in\mathbb{R}_+, \end{cases}$$

numerically. This procedure is carefully explained in Chapter 4. Remembering that we have an explicit expression (5.3) for $p_i(T,y)$ we can compute the right hand side of (5.11) by using numerical integration. To be more precise, we use the `quad`-function in Matlab which is an adaptive Simpson's rule.

In order to check the relation (5.11) we let A be an interval, $S_0 = 2600$, $K = 2500$, and $T_k = k/252$, $k = 0,...,25$, $N = 3$, $\varepsilon = 1/252$, $\delta = 2/252$, $\bar{\sigma} = 0.3$, $(\bar{\sigma}_1,\bar{\sigma}_2,\bar{\sigma}_3) = (0.2,0.3,0.4)$, $(\lambda_1,\lambda_2,\lambda_3) = (1/4,1/2,1/4)$. Moreover, γ_i, $i = 1,2,3$ are the affine functions

$$\gamma_i(t) = \bar{\sigma} + (t-\varepsilon)\frac{\bar{\sigma}_i - \bar{\sigma}}{\delta - \varepsilon}, \quad t\in[\varepsilon,\delta], i = 1,2,3.$$

The results are displayed in Table 5.1 where the left and right hand side of the relation (5.11) are denoted LHS and RHS respectively and the difference is the absolute difference. The differences are readily seen to be very small.

Time	LHS	RHS	Difference
T_0	1	1	0
T_1	0.9975	0.9996	0.0021
T_2	0.9853	0.9924	0.0071
T_3	0.9690	0.9759	0.0069
T_4	0.9499	0.9544	0.0045
T_5	0.9293	0.9310	0.0017
T_6	0.9081	0.9072	0.0009
T_7	0.8869	0.8840	0.0029
T_8	0.8661	0.8616	0.0045
T_9	0.8460	0.8404	0.0056
T_{10}	0.8267	0.8203	0.0064
T_{11}	0.8082	0.8013	0.0070
T_{12}	0.7907	0.7833	0.0073
T_{13}	0.7740	0.7664	0.0076
T_{14}	0.7581	0.7504	0.0077
T_{15}	0.7431	0.7352	0.0078
T_{16}	0.7288	0.7209	0.0079
T_{17}	0.7153	0.7073	0.0079
T_{18}	0.7024	0.6945	0.0079
T_{19}	0.6901	0.6822	0.0079
T_{20}	0.6785	0.6706	0.0079
T_{21}	0.6674	0.6595	0.0079
T_{22}	0.6569	0.6489	0.0080
T_{23}	0.6468	0.6388	0.0080
T_{24}	0.6372	0.6291	0.0081
T_{25}	0.6280	0.6199	0.0081

(a) $A = [2400, 2700]$

Time	LHS	RHS	Difference
T_0	0	0	0
T_1	0.0014	0.0002	0.0011
T_2	0.0072	0.0044	0.0028
T_3	0.0142	0.0126	0.0015
T_4	0.0216	0.0219	0.0002
T_5	0.0291	0.0308	0.0017
T_6	0.0361	0.0387	0.0026
T_7	0.0425	0.0457	0.0031
T_8	0.0482	0.0516	0.0033
T_9	0.0533	0.0567	0.0033
T_{10}	0.0578	0.0610	0.0031
T_{11}	0.0618	0.0647	0.0029
T_{12}	0.0652	0.0679	0.0026
T_{13}	0.0682	0.0706	0.0023
T_{14}	0.0709	0.0729	0.0020
T_{15}	0.0732	0.0748	0.0016
T_{16}	0.0752	0.0765	0.0013
T_{17}	0.0769	0.0779	0.0009
T_{18}	0.0785	0.0791	0.0006
T_{19}	0.0798	0.0801	0.0002
T_{20}	0.0810	0.0809	0.0001
T_{21}	0.0821	0.0816	0.0004
T_{22}	0.0831	0.0822	0.0008
T_{23}	0.0839	0.0827	0.0012
T_{24}	0.0847	0.0830	0.0017
T_{25}	0.0855	0.0833	0.0021

(b) $A = [2700, 2800]$

Table 5.1: Two different tests of the relation (5.11).

In the the Brigo-Mercurio log-normal mixture model, the time zero price of a call option is immediate and is simply equal to a convex combination of Black-Scholes call option prices. If we denote by c_{BM} the call option price in the Brigo-Mercurio model and by c_{BS} the call option price in the Black-Scholes model, then

$$
\begin{aligned}
c_{BM}(0,S_0,K,T) &= e^{-rT}E[(S(T)-K)^+] = e^{-rT}\int_0^\infty (y-K)^+ p(T,y)dy \\
&= e^{-rT}\int_0^\infty (y-K)^+ \sum_{i=1}^N \lambda_i p_i(T,y)dy \\
&= \sum_{i=1}^N \lambda_i e^{-rT}\int_0^\infty (y-K)^+ p_i(T,y)dy \\
&= \sum_{i=1}^N \lambda_i e^{-rT}E[(S_i(T)-K)^+] \\
&= \sum_{i=1}^N \lambda_i c_{BS}(0,S_0,K,T;\eta_i), \qquad (5.12)
\end{aligned}
$$

where

$$\eta_i := \frac{V_i(T)}{\sqrt{T}}, \quad i=1,...,N.$$

If c_{BM} is as in (5.12) we sometimes write

$$c_{BM}(0,S_0,K,T) = c_{BM}(0,S_0,K,T;\eta_1,...,\eta_N).$$

Recall from Chapter 3.1 that for fixed $i \in \{1,...,N\}$,

$$c_{BS}(0,S_0,K,T,\eta_i) = S_0\Phi(d_1) - Ke^{-rT}\Phi(d_2)$$

where

$$d_1 = \frac{\ln\frac{s}{K} + \left(r+\frac{1}{2}\eta_i^2\right)T}{\eta_i\sqrt{T}}$$

and

$$d_2 = \frac{\ln\frac{s}{K} + \left(r-\frac{1}{2}\eta_i^2\right)T}{\eta_i\sqrt{T}}.$$

Consequently we get the following expression for the time zero call option price in the Brigo-Mercurio model

$$
\begin{aligned}
c_{BM}(0,S_0,K,T) = \sum_{i=1}^N \Bigg[& S_0\Phi\left(\frac{\ln\frac{S_0}{K} + \left(r+\frac{1}{2}\eta_i^2\right)T}{\eta_i\sqrt{T}}\right) \\
& - Ke^{-rT}\Phi\left(\frac{\ln\frac{S_0}{K} + \left(r-\frac{1}{2}\eta_i^2\right)T}{\eta_i\sqrt{T}}\right)\Bigg]. \qquad (5.13)
\end{aligned}
$$

The option price (5.13) leads to smiles in the implied volatility structure. An example of the smiley shape is illustrated in Figure 5.3.

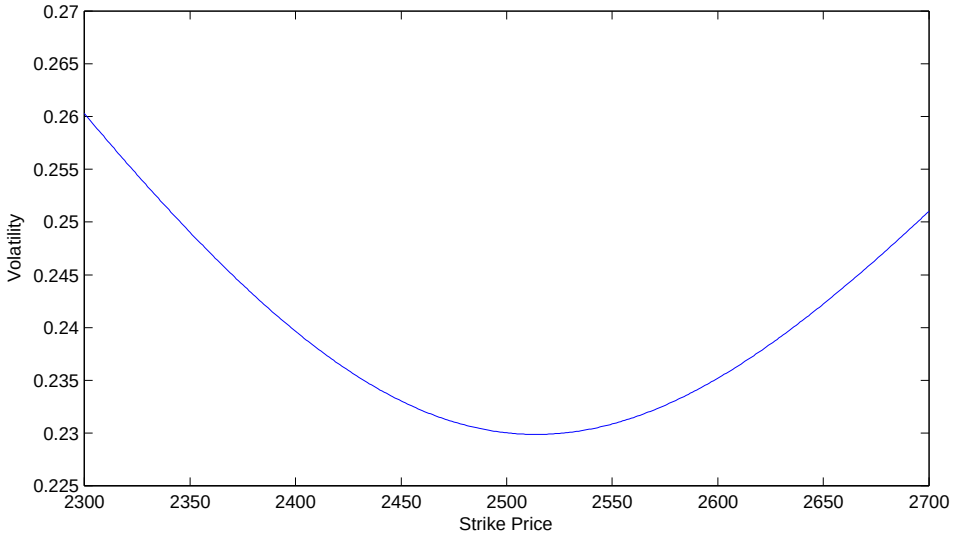

Figure 5.3: The volatility implied by equation (5.13). We have set $S_0 = 2500$, $r = 0.01$, $T = 44/252$, $N = 3$, $(\eta_1, \eta_2, \eta_3) = (0.5, 0.1, 0.2)$ and $(\lambda_1, \lambda_2, \lambda_3) = (0.2, 0.3, 0.5)$

5.3 Smiles in the implied volatility structure

In this section we prove that the volatility implied by the option price (5.12) has a local minimum at the underlying forward price $\bar{K} = S_0 e^{rT}$. There is a unique so called implied volatility, σ_{imp}, implicitly defined by the equation

$$c_{BS}(0, S_0, K, T, \sigma_{imp}) = \sum_{i=1}^{N} \lambda_i c_{BS}(0, S_0, K, T, \eta_i). \tag{5.14}$$

If $N = 1$ the result is well known and reduces to the classical case, so in the following we assume that $N \geq 2$ and that $\lambda_1, ..., \lambda_N > 0$ where $\lambda_1 + ... + \lambda_N = 1$.

To prove that $\sigma_{imp}(K)$ has a local minimum at $K = \bar{K}$ it is enough to prove that

$$\frac{d\sigma_{imp}}{dK}(S_0 e^{rT}) = 0$$

and

$$\frac{d^2\sigma_{imp}}{dK^2}(S_0 e^{rT}) > 0.$$

From now on we write $\sigma(K)$ instead of $\sigma_{imp}(K)$. Differentiating both sides of (5.14) with respect to K we get

$$\frac{\partial c_{BS}}{\partial K}(0,S_0,K,T,\sigma(K)) + \frac{\partial c_{BS}}{\partial \sigma}(0,S_0,K,T,\sigma(K))\frac{d\sigma}{dK}(K) = \sum_{i=1}^{N}\lambda_i \frac{\partial c_{BS}}{\partial K}(0,S_0,K,T,\eta_i). \tag{5.15}$$

In the Black-Scholes model we know that

$$\frac{\partial c_{BS}}{\partial K}(0,S_0,K,T,\sigma) = -e^{-rT}\Phi\left(\frac{\ln\frac{S_0}{K} + \left(r-\frac{\sigma^2}{2}\right)T}{\sigma\sqrt{T}}\right)$$

and

$$\frac{\partial c_{BS}}{\partial \sigma}(0,S_0,K,T,\sigma) = S_0\sqrt{T}\varphi\left(\frac{\ln\frac{S_0}{K} + \left(r+\frac{\sigma^2}{2}\right)T}{\sigma\sqrt{T}}\right).$$

Especially noting that $\frac{\partial c_{BS}}{\partial \sigma} > 0$ we can rewrite equation (5.15) in the following way

$$\frac{d\sigma}{dK}(K) = \frac{\sum_{i=1}^{N}\lambda_i \frac{\partial c_{BS}}{\partial K}(0,S_0,K,T,\eta_i) - \frac{\partial c_{BS}}{\partial K}(0,S_0,K,T,\sigma(K))}{\frac{\partial c_{BS}}{\partial \sigma}(0,S_0,K,T,\sigma(K))}$$

$$= -e^{-rT}\frac{\sum_{i=1}^{N}\lambda_i\Phi\left(\frac{\ln\frac{S_0}{K}+\left(r-\frac{\eta_i^2}{2}\right)T}{\eta_i\sqrt{T}}\right) - \Phi\left(\frac{\ln\frac{S_0}{K}+\left(r-\frac{\sigma^2(K)}{2}\right)T}{\sigma(K)\sqrt{T}}\right)}{S_0\sqrt{T}\varphi\left(\frac{\ln\frac{S_0}{K}+\left(r+\frac{\sigma^2(K)}{2}\right)T}{\sigma(K)\sqrt{T}}\right)}.$$

Now if $K=\bar{K}$ we get

$$\frac{d\sigma}{dK}(\bar{K}) = -e^{-rT}\frac{\sum_{i=1}^{N}\lambda_i\Phi\left(-\frac{\eta_i}{2}\sqrt{T}\right) - \Phi\left(-\frac{\sigma(\bar{K})}{2}\sqrt{T}\right)}{S_0\sqrt{T}\varphi\left(\frac{\sigma(\bar{K})}{2}\sqrt{T}\right)} = 0$$

since the equation (5.14) yields

$$0 = \sum_{i=1}^{N}\lambda_i c_{BS}(0,S_0,\bar{K},T,\eta_i) - c_{BS}(0,S_0,\bar{K},T,\sigma(\bar{K}))$$
$$= \sum_{i=1}^{N}\lambda_i\Phi\left(-\frac{\eta_i}{2}\sqrt{T}\right) - \Phi\left(-\frac{\sigma(\bar{K})}{2}\sqrt{T}\right). \tag{5.16}$$

This proves that $\frac{d\sigma}{dK}(\bar{K}) = 0$. If we differentiate the relation (5.15) with respect to K again we get

$$\begin{aligned}\frac{d^2\sigma}{dK^2}(\bar{K}) &= \frac{\sum_{i=1}^{N} \lambda_i \frac{\partial^2 c_{BS}}{\partial K^2}(0, S_0, \bar{K}, T, \eta_i) - \frac{\partial^2 c_{BS}}{\partial K^2}(0, S_0, \bar{K}, T, \sigma(\bar{K}))}{\frac{\partial c_{BS}}{\partial \sigma}(0, S_0, \bar{K}, T, \sigma(\bar{K}))} \\ &= e^{-rT} \frac{\sum_{i=1}^{N} \frac{\lambda_i}{\bar{K}\sigma_i\sqrt{T}} \varphi\left(-\frac{\eta_i}{2}\sqrt{T}\right) - \frac{1}{\bar{K}\sigma(\bar{K})\sqrt{T}} \varphi\left(-\frac{\sigma(\bar{K})}{2}\sqrt{T}\right)}{S_0\sqrt{T}\varphi\left(\frac{\sigma(\bar{K})}{2}\sqrt{T}\right)}.\end{aligned}$$

Now we see that $\frac{d^2\sigma}{dK^2}(\bar{K}) > 0$ if and only if

$$\sum_{i=1}^{N} \lambda_i \frac{\varphi\left(-\frac{\eta_i}{2}\sqrt{T}\right)}{\bar{K}\eta_i\sqrt{T}} > \frac{\varphi\left(-\frac{\sigma(\bar{K})}{2}\sqrt{T}\right)}{\bar{K}\sigma(\bar{K})\sqrt{T}} \tag{5.17}$$

and introducing

$$\begin{cases} x_i = -\dfrac{\eta_i}{2}\sqrt{T}, \quad i = 1, ..., N, \\ \bar{x} = -\dfrac{\sigma(\bar{K})}{2}\sqrt{T}, \end{cases}$$

the inequality (5.17) becomes

$$\frac{\varphi(\bar{x})}{\bar{x}} > \sum_{i=1}^{N} \lambda_i \frac{\varphi(x_i)}{x_i}.$$

In order to prove this inequality it suffices to prove the existence of a real constant ρ such that

$$\rho\left(\Phi(\bar{x}) - \Phi(x_i)\right) \leq \frac{\varphi(\bar{x})}{\bar{x}} - \frac{\varphi(x_i)}{x_i}, \quad i = 1, ..., N. \tag{5.18}$$

Since if such a ρ exist we can multiply both sides of the equation by λ_i and sum over $i = 1, ..., N$ to get

$$\rho\left(\Phi(\bar{x}) - \sum_{i=1}^{N} \lambda_i \Phi(x_i)\right) \leq \frac{\varphi(\bar{x})}{\bar{x}} - \sum_{i=1}^{N} \lambda_i \frac{\varphi(x_i)}{x_i}$$

Remembering equation (5.16) we have

$$\Phi(\bar{x}) - \sum_{i=1}^{N} \lambda_i \Phi(x_i) = 0 \tag{5.19}$$

and thus

$$\frac{\varphi(\bar{x})}{\bar{x}} \geq \sum_{i=1}^{N} \lambda_i \frac{\varphi(x_i)}{x_i} \tag{5.20}$$

where we shall prove that the inequality must be strict. It is no restriction to assume that $x_1 < x_2 < ... < x_s \leq \bar{x} \leq x_{s+1} < ... < x_N < 0$. Indeed, if $\bar{x} < x_1$ or $\bar{x} > x_N$ the equation (5.19) would not hold since Φ is a strictly increasing function. If equality occurs i.e. $\bar{x} = x_s$ or $\bar{x} = x_{s+1}$ then the equation (5.18) is trivially satisfied. Therefore we assume that strict inequality holds. Further, since Φ is a strictly increasing function we can write equation (5.18) as

$$\begin{cases} \rho \leq \dfrac{\frac{\varphi(\bar{x})}{\bar{x}} - \frac{\varphi(x_i)}{x_i}}{\Phi(\bar{x}) - \Phi(x_i)}, & i = 1, ..., s \\ \\ \rho \geq \dfrac{\frac{\varphi(\bar{x})}{\bar{x}} - \frac{\varphi(x_i)}{x_i}}{\Phi(\bar{x}) - \Phi(x_i)}, & i = s+1, ..., N. \end{cases}$$

This system has a solution ρ if and only if

$$\min_{i=1,...,s} \frac{\frac{\varphi(\bar{x})}{\bar{x}} - \frac{\varphi(x_i)}{x_i}}{\Phi(\bar{x}) - \Phi(x_i)} \geq \max_{i=s+1,...,N} \frac{\frac{\varphi(\bar{x})}{\bar{x}} - \frac{\varphi(x_i)}{x_i}}{\Phi(\bar{x}) - \Phi(x_i)}.$$

This inequality must hold since the map

$$(-\infty, 0) \backslash \{\bar{x}\} \ni z \longmapsto \frac{\frac{\varphi(\bar{x})}{\bar{x}} - \frac{\varphi(z)}{z}}{\Phi(\bar{x}) - \Phi(z)} \tag{5.21}$$

is strictly decreasing. To see why it is strictly decreasing we note that

$$\frac{d}{dz} \frac{\frac{\varphi(\bar{x})}{\bar{x}} - \frac{\varphi(z)}{z}}{\Phi(\bar{x}) - \Phi(z)}$$

$$= \left[\big(\Phi(\bar{x}) - \Phi(z)\big)\Big(1 + \frac{1}{z^2}\Big) + \Big(\frac{\varphi(\bar{x})}{\bar{x}} - \frac{\varphi(z)}{z}\Big) \right] \frac{\varphi(z)}{\big(\Phi(\bar{x}) - \Phi(z)\big)^2}$$

is negative if and only if

$$g(\bar{x}) := \big(\Phi(\bar{x}) - \Phi(z)\big)\Big(1 + \frac{1}{z^2}\Big) + \Big(\frac{\varphi(\bar{x})}{\bar{x}} - \frac{\varphi(z)}{z}\Big) < 0.$$

This is readily seen to hold true since

$$\begin{aligned} g'(\bar{x}) &= \varphi(\bar{x})\Big(1 + \frac{1}{z^2}\Big) + \frac{\varphi'(\bar{x})\bar{x} - \varphi(\bar{x})}{\bar{x}^2} \\ &= \varphi(\bar{x})\Big(\frac{\bar{x}^2 - z^2}{\bar{x}^2 z^2}\Big) \\ &= \frac{\varphi(\bar{x})}{\bar{x}^2 z^2}(\bar{x} + z)(\bar{x} - z) \end{aligned}$$

and

$$g(z) = 0.$$

Finally we prove that the inequality in (5.20) must be strict. Assume that equality holds, then we would also have equality in the equations (5.18) which implies that

$$\rho = \frac{\frac{\varphi(\bar{x})}{\bar{x}} - \frac{\varphi(x_1)}{x_1}}{\Phi(\bar{x}) - \Phi(x_1)} = \frac{\frac{\varphi(\bar{x})}{\bar{x}} - \frac{\varphi(x_N)}{x_N}}{\Phi(\bar{x}) - \Phi(x_N)}$$

which cannot be true since $x_1 < x_N < 0$ and the map (5.21) is strictly decreasing in $(-\infty, 0)$. This completes the proof that $\frac{d^2\sigma}{dK^2}(\bar{K}) > 0$.

Chapter 6

Method & Results

The aim of this Chapter is to first describe in detail how the implementation of the model was done, how it was calibrated and how the hedging was performed. Then we will present the results from the hedging and compare it with the Black-Scholes model. We begin by presenting the market data that will be used.

6.1 Data description

The underlying price process consists of daily closing prices of a European stock index called the Euro Stoxx 50 [2] or SX5E for short. The index consists of 50 stocks from 12 Eurozone countries: Austria, Belgium, Finland, France, Germany, Greece, Ireland, Italy, Luxembourg, the Netherlands, Portugal, and Spain. The index also ranges over a variety of different sectors like banks, oil & gas, chemicals, insurance, telecommunications etc. The currency is Euro.

The interest rate is the 1-month Euro Interbank Offered Rate [9] or EURIBOR for short. The rate is set by a representative collection of European banks in the way that each bank presents its estimate of what a prime bank would quote another prime bank for interbank term deposits (e.g. bonds) within the euro-zone. The rates are quoted in a actual/360 day-count convention meaning that a year has 360 days but each month is treated normally. So the rate during January would be 31/360 amount of rate.

The option is the Euro Stoxx 50 Index option traded on Eurex Deutschland. Eurex Deutschland is a large electronic trading platform which issues many different kinds of derivatives. The contract length considered is 1 and 2 months and the contracts mature on the third Friday in the respective month of maturity. See [10] for more contract specifications.

The option prices are quoted in terms of implied volatility together with a level of moneyness. Moneyness is a measure of how the stock price relates to a strike price on a particular day. We must emphasize that it is not a strike

price in the way we usually think of it but rather a new strike price every day. For example, a moneyness of 110% on a given day means that $S/K = 1.1$ where S is the spot price on the day in question. We have 9 different levels of moneyness every day which equivalently means that we have 9 different strikes every day, namely aS, $a = 0.8, 0.9, 0.95, 0.975, 1, 1.025, 1.05, 1.1, 1.2$.

We convert the implied volatilities into call option prices using the Black-Scholes formula. This means that for each day we will have 9 different call option prices corresponding to 9 different strike prices. When considering a call option contract we need to have a fixed strike price over the whole contract time. At the first day of a call option contract we have 9 different strikes which we hold fixed over the whole length of the contract by interpolating over each day's strike prices. An example of this is illustrated in Figure 6.1 where we construct a call option contract that start at the money, i.e. $K = S(0)$. We will always use spline interpolation for this procedure.

Note that if the stock price fluctuates too much the interpolation in contracts that starts deep in the money, e.g. $K = 1.2S(0)$, or deep out of the money, e.g. $K = 0.8S(0)$, might not be very precise.

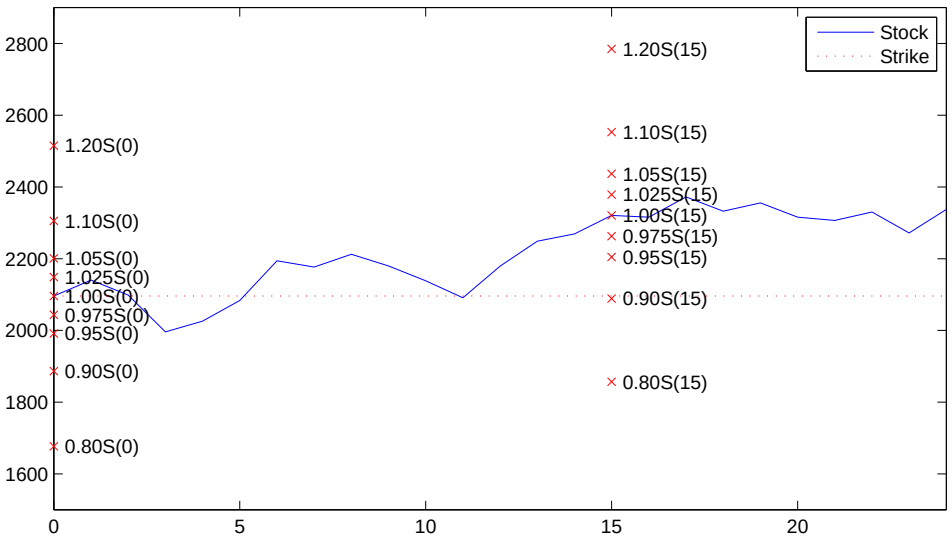

Figure 6.1: Illustration of the construction of an at the money call option contract by interpolation.

For the 1-month options we have 12 different contract periods, which are presented in Table 6.2. The start date of the option is the date when the option is issued and the settlement date is the maturity date of the option. Note also that there is one month missing. This is because that particular period was very extreme in the sense that the index dropped almost 20%. This in turn generates too big errors in the interpolation and therefore we drop this extreme period.

Period	Start Date	Settlement Date
1	18-Oct-2010	19-Nov-2010
2	22-Nov-2010	17-Dec-2010
3	20-Dec-2010	21-Jan-2011
4	24-Jan-2011	18-Feb-2011
5	21-Feb-2011	18-Mar-2011
6	21-Mar-2011	15-Apr-2011
7	18-Apr-2011	20-May-2011
8	23-May-2011	17-Jun-2011
9	20-Jun-2011	15-Jul-2011
10	22-Aug-2011	16-Sep-2011
11	19-Sep-2011	21-Oct-2011
12	24-Oct-2011	18-Nov-2011

Table 6.1: The different contract periods for the 1-month call options.

For the 2-month options we have 5 different contract periods. Again, since the index dropped around 20% during the period July–August in 2011 the corresponding contract period will be dropped. We are left with the following 5 periods.

Period	Start Date	Settlement Date
1	18-Oct-2010	17-Dec-2010
2	20-Dec-2010	18-Feb-2011
3	21-Feb-2011	15-Apr-2011
4	18-Apr-2011	17-Jun-2011
5	22-Aug-2011	21-Oct-2011

Table 6.2: The different contract periods for the 2-month call options.

6.2 Hedging & Hedging Error

In Section 5 we concluded that, if we want to compute a call price in the log-normal mixture model at time zero it is simply a convex combination of Black-Scholes call prices at time zero. If we want to compute a call price at any other point in time we can use Monte Carlo methods or alternatively the Feynman-Kac connection and solve a partial differential equation using standard numerical methods. The latter approach is the one we use in this thesis. Remember that the we have the following dynamics for the price process:

$$\begin{cases} dS(t) = rS(t)dt + \sigma(t, S(t))S(t)dW(t) \\ S(0) = S_0 \end{cases}$$

with

$$\sigma(t,y) = \sqrt{\frac{\sum_{i=1}^{N} \lambda_i \sigma(t)_i^2 \frac{1}{V_i(t)} \exp\left\{-\frac{1}{2V_i^2(t)}\left[\ln\frac{y}{S_0} - rt + \frac{1}{2}V_i^2(t)\right]^2\right\}}{\sum_{i=1}^{N} \lambda_i \frac{1}{V_i(t)} \exp\left\{-\frac{1}{2V_i^2(t)}\left[\ln\frac{y}{S_0} - rt + \frac{1}{2}V_i^2(t)\right]^2\right\}}},$$

and

$$V_i(t) = V(t,\sigma_i) = \sqrt{\int_0^t \sigma_i^2(s)ds}, \quad i = 1, ..., N.$$

The time t price of a European style call option paying $(S(T)-K)^+$ at time of maturity is $V(t) = v(t, S(t))$ where

$$v(t,x) = E\big[e^{-r(T-t)}(S(T)-K)^+ | S(t) = x\big]$$

Thus by the Feynman-Kac connection v must satisfy the following partial differential equation

$$\begin{cases} \dfrac{\partial v}{\partial t} + rx\dfrac{\partial v}{\partial x} + \dfrac{1}{2}x^2\sigma^2(t,x)\dfrac{\partial^2 v}{\partial x^2} - rv = 0, \quad (t,x) \in [0,T[\times\mathbb{R}_+, \\ v(T,x) = (x-K)^+, \quad x \in \mathbb{R}_+, \end{cases} \tag{6.1}$$

We described in detail how to solve equation (6.1) numerically in Chapter 4.

The aim is to see how well the Brigo-Mercurio model hedges compared to the Black-Scholes model. To this end we will use a so called delta hedging strategy. In Chapter 3 we proved the existence of such a strategy for a local volatility model. If we rebalance the hedging portfolio continuously it is possible to hedge perfectly i.e. the value of the hedging portfolio and the value of the call option will always be equal. However, in practice it is only possible to rebalance the hedging portfolio in discrete time. This leads to a so called call hedging error.

Suppose we have a equidistant time grid $0 = t_0 < t_1 < ... < t_n = T$ with $t_1 - t_0 = k$. Let $\hat{c} = \hat{c}(t, S(t), T, K)$ denote the real market price at time t of the call option with strike K and maturity T and let $\Delta(t) = v'_x(t, S(t))$. Then we proceed in the following steps[1]:

1. Define $\text{cash}(t_0)$ by $\hat{c}(t_0, S(t_0), T, K) = \Delta(t_0)S(t_0) + \text{cash}(t_0)$.
2. Set $\Pi(t_0) = \Delta(t_0)S(t_0) + \text{cash}(t_0)$.
3. Define $\Pi(t_1) = \Delta(t_0)S(t_1) + \text{cash}(t_0)e^{rk}$.
4. Define $\text{cash}(t_1)$ by $\Pi(t_1) = \Delta(t_1)S(t_1) + \text{cash}(t_1)$.

[1]We want to point out that we assume no transaction costs when rebalancing the hedging portfolio Π.

5. Define $\Pi(t_2) = \Delta(t_1)S(t_2) + \text{cash}(t_1)e^{rk}$.

We continue in this way until we reach time T and then the hedging error is defined as the absolute difference, at time T, between the value of the hedging portfolio Π and the value of the call option, viz.

$$|\Pi(T) - (S(T) - K)^+|.$$

Remember that for each contract period we have 9 different options corresponding to 9 different strike prices. Therefore, the error we are going to examine is the mean of the hedging errors for the 9 different options i.e.

$$\frac{1}{9}\sum_{i=1}^{9} |\Pi_i(T) - (S(T) - K_i)^+|.$$

This quantity is interesting because it says something about how good the model hedges a variety of different options i.e. options that are in the money as well as out of the money.

Note that in the above presented delta hedging scheme we choose $\sigma(t, y)$ at time t_0 and then we keep it fixed. Choosing $\sigma(t, y)$ is equivalent to choosing $\bar{\sigma}$, $\gamma_1, ..., \gamma_N$, $\bar{\sigma}_1, ..., \bar{\sigma}_N$ and $\lambda_1, ..., \lambda_N$. In the next section we describe ways of choosing these parameters in a good way. The above hedging scheme will be called hedging scheme A for short.

Now consider a slightly different way of hedging. It is similar to the hedging scheme A presented above but each day when we choose a new delta we also choose a new $\sigma(t, y)$ by choosing the parameters $\bar{\sigma}$, $\gamma_1, ..., \gamma_N$, $\bar{\sigma}_1, ..., \bar{\sigma}_N$ and $\lambda_1, ..., \lambda_N$ in some optimal way. This way of hedging seems more natural from an investor's point of view since it is sensible that you would want to update σ when computing the delta every day. We will call this hedging scheme B.

6.3 Calibration

Before we can apply the hedging schemes we must choose a way to determine the parameters in the Black-Scholes model and in the Brigo-Mercurio model. In the Black-Scholes model we have only one parameter σ but in the Brigo-Mercurio model we have the parameters $\bar{\sigma}$, $\bar{\sigma}_1, ..., \bar{\sigma}_N$ and $\lambda_1, ..., \lambda_{N-1}$ since $\lambda_1 + ... + \lambda_N = 1$. One could also consider $\gamma_1, ..., \gamma_N$, ε and δ as parameters, but in the following, if not stated otherwise, $\varepsilon = 1/252$, $\delta = 2/252$ and for each $i \in \{1, ..., N\}$, γ_i is the line segment between $\bar{\sigma}$ and $\bar{\sigma}_i$, that is:

$$\gamma_i(t) = \bar{\sigma} + (t - \varepsilon)\frac{\bar{\sigma}_i - \bar{\sigma}}{\delta - \varepsilon}, \quad t \in [\varepsilon, \delta].$$

In Section 6.4.3 we investigate the dependence of ε and δ.

In the Black-Scholes model we calibrate the parameter σ by minimizing the absolute difference between the Black-Scholes call price and the market call price, viz.

$$\min_{\sigma\in\mathbb{R}_+} \frac{1}{9}\sum_{i=1}^{9} |c_{BS}(t, S(t), K_i, T; \sigma) - \hat{c}(t, S(t), K_i, T)|. \tag{6.2}$$

The optimization problem (6.2) is solved using Matlab's function `fmincon`.

The parameter $\bar{\sigma}$ in the Brigo-Mercurio model will always be chosen as the optimal parameter in (6.2). We will describe two methods for how to calibrate the remaining parameters, $\bar{\sigma}_1, ..., \bar{\sigma}_N$ and $\lambda_1, ..., \lambda_{N-1}$, in the Brigo-Mercurio model. The first method is to minimize the sum of the absolute differences between the Brigo-Mercurio call option price c_{BM} and the market call option price $\hat{c}$, viz.

$$\min_{\substack{\lambda_1,...,\lambda_N\in[0,1]\\ \lambda_1+...+\lambda_N=1\\ \bar{\sigma}_1,...,\bar{\sigma}_N\in\mathbb{R}_+}} \frac{1}{9}\sum_{i=1}^{9} |c_{BM}(0, S(0), K_i, T; \eta_1(\bar{\sigma}_1), ..., \eta_N(\bar{\sigma}_N)) - \hat{c}(0, S(0), K_i, T)|. \tag{6.3}$$

The optimization problem (6.3) is also solved using Matlab's function `fmincon`. We choose $\bar{\sigma}_1, ..., \bar{\sigma}_N$ and $\lambda_1, ..., \lambda_{N-1}$ as the optimal parameters in (6.3) and in the sequel, if not stated otherwise, $N = 3$.

Given the optimal parameters in the Brigo-Mercurio model, the next step is to calculate $\Delta(t_i)$, $i = 0, ..., n$. For the hedging scheme A, if $t = t_0$, we simply use the optimal parameters and then differentiate the relation (5.12) with respect to S_0 to obtain $\Delta(t_0)$ in the Brigo-Mercurio model. If $t \geq t_1$ we can use our PDE-solution and numerical differentiation to calculate $\Delta(t_i)$ with the optimal parameters for $i = 1, ..., n$.

Note that for the hedging scheme B above we must perform the calibrations (6.2) and (6.3) at every time point t_i, $i = 0, ..., n$. However, calculating $\Delta(t_i)$, $i = 1, ..., n$, in the Brigo-Mercurio model is simple because in each time step it is as if we stand at the starting point, i.e. in each time step we can calculate $\Delta(t_i)$, $i = 1, ..., n$, by differentiating the relation (5.12) with respect to S_0.

Above we have calibrated the model to market data by minimizing the difference between model and market prices. It is not self-evident that this is a good method when we are interested in hedging errors. We will propose another method of calibration, namely to minimize the difference between the price of a hedging portfolio and the market call price.

Assume we want to calibrate the Brigo-Mercurio model in time t_m i.e. we want to find optimal parameters at time t_m. We then let $i \in \{1, ..., 9\}$ and

set up a delta hedging portfolio at time t_{m-1} by first defining $\text{cash}_i(t_{m-1})$ by

$$\hat{c}_i(t_{m-1}, S(t_{m-1}), K_i, T) = \Delta_i(t_{m-1})S(t_{m-1}) + \text{cash}_i(t_{m-1}).$$

We define the hedging portfolio at t_{m-1} by

$$\Pi_i(t_{m-1}) = \Delta_i(t_{m-1})S(t_{m-1}) + \text{cash}_i(t_{m-1})$$

and setting $\Pi_i(t_m) = \Delta_i(t_{m-1})S(t_m) + \text{cash}_i(t_{m-1})e^{rk}$ we are interested in the minimum of the mean of the absolute errors

$$\min_{\substack{\lambda_1,\ldots,\lambda_N\in[0,1]\\ \lambda_1+\ldots+\lambda_N=1\\ \bar{\sigma}_1,\ldots,\bar{\sigma}_N\in\mathbb{R}_+}} \frac{1}{9}\sum_{i=1}^{9} |\Pi_i(t_m) - \hat{c}(t_m, S(t_m), K_i, T)| \tag{6.4}$$

where $\hat{c}$ denotes the market price of the call option.

6.4 Results

We begin by examining the hedging error from using the hedging scheme A for both 1-month and 2-month call option.

6.4.1 Hedging Scheme A

In Table 6.3 we present the absolute hedging errors when hedging the 1-month options with the hedging scheme A.

Period	Black-Scholes	Brigo-Mercurio
1	81.30	77.12
2	47.84	43.72
3	30.34	34.34
4	97.32	94.14
5	57.74	64.28
6	128.07	125.16
7	51.32	60.57
8	77.61	91.81
9	72.64	57.02
10	76.92	52.80
11	43.30	47.82
12	139.59	132.00

Table 6.3: The absolute hedging errors for each 1-month contract period when using hedging scheme A.

If we examine the relative differences i.e. the hedging error in the Brigo-Mercurio model minus the hedging error in the Black-Scholes model divided by the hedging error in the Black-Scholes model we get the results in Table 6.4. A negative percentage means that we gained that much in comparison with the Black-Scholes model.

Period	Relvative difference
1	-5%
2	-9%
3	+13%
4	-3%
5	+11%
6	-2%
7	+18%
8	+19%
9	-22%
10	-31%
11	+10%
12	-5%

Table 6.4: The absolute hedging errors for each 1-month contract period when using hedging scheme A.

We can conclude that if one would have used the Brigo-Mercurio model during the whole year the error would have been reduced by about 3% compared to the Black-Scholes model. Figure 6.2 displays a 1 month delta hedging strategy for the Brigo-Mercurio and the Black-Scholes model. The option that has been hedged is an at-the-money option meaning that at time zero the strike is equal to the stock price.

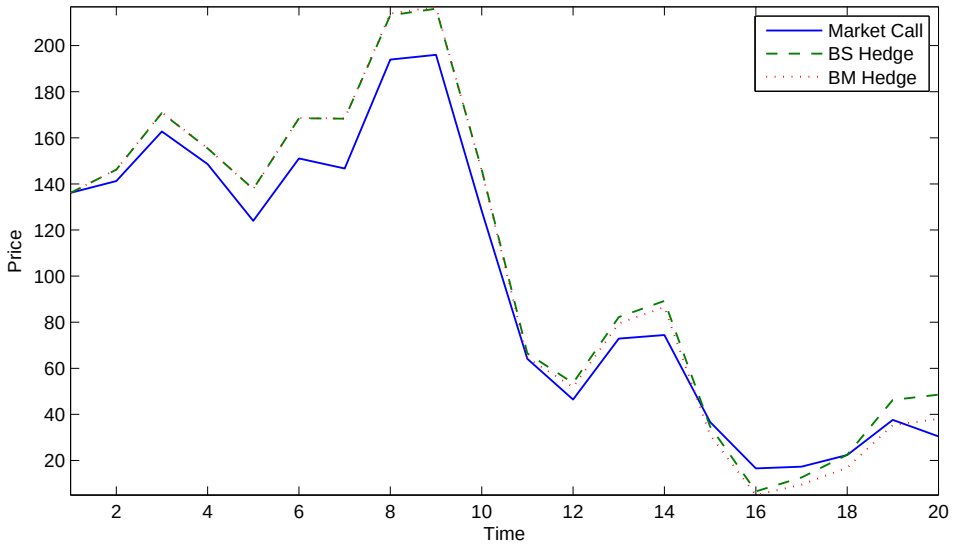

Figure 6.2: This figure displays two delta hedging portfolios together with the market call price. One has been hedged with the aid of the Black-Scholes delta and the other with the aid of the Brigo-Mercurio delta.

In Figure 6.3 we can see how the $\Delta(t)$ changed over time during Period 7 in both the Black-Scholes model and in the Brigo-Mercurio model.

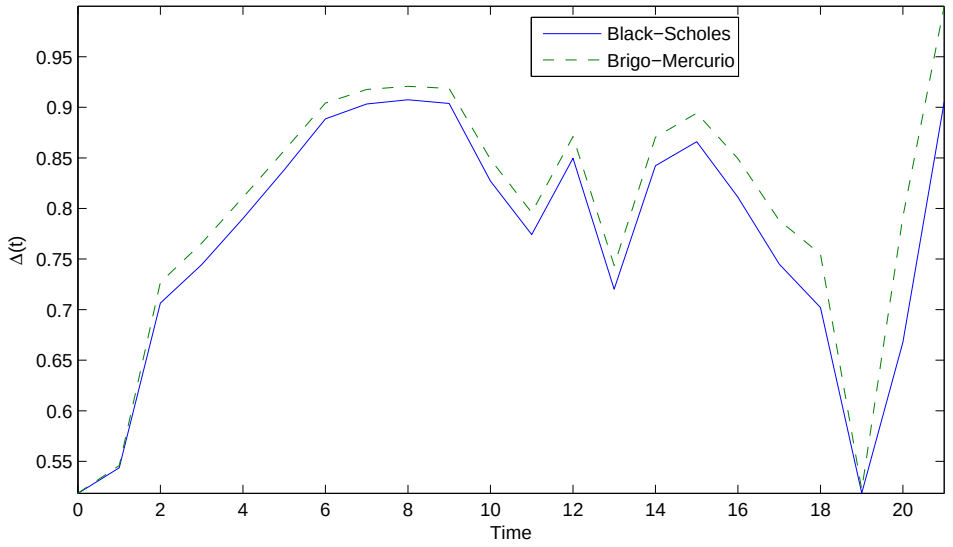

Figure 6.3: This figure displays $\Delta(t)$ in both the Black-Scholes model and the Brigo-Mercurio model during Period 7.

The next step is to perform the same analysis of the hedging error for the 2-month options. The absolute hedging errors are presented in Table 6.5 and in Table 6.6 we present the relative differences.

Period	Black-Scholes	Brigo-Mercurio
1	159.36	155.60
2	129.03	130.51
3	133.60	130.03
4	81.21	78.81
5	64.15	78.05

Table 6.5: The absolute hedging errors for each 2-month contract period when using hedging scheme A.

Period	Relvative difference
1	-2%
2	+1%
3	-3%
4	-3%
5	+22%

Table 6.6: The relative hedging errors for each 2-month contract period when using hedging scheme A.

We can conclude that if one would have used the Brigo-Mercurio model during the whole year one would have increased the error about 1% compared with Black-Scholes model. Figure 6.4 displays a 2 month delta hedging strategy for Brigo-Mercurio and Black-Scholes model. The option that has been hedged is an at-the-money option.

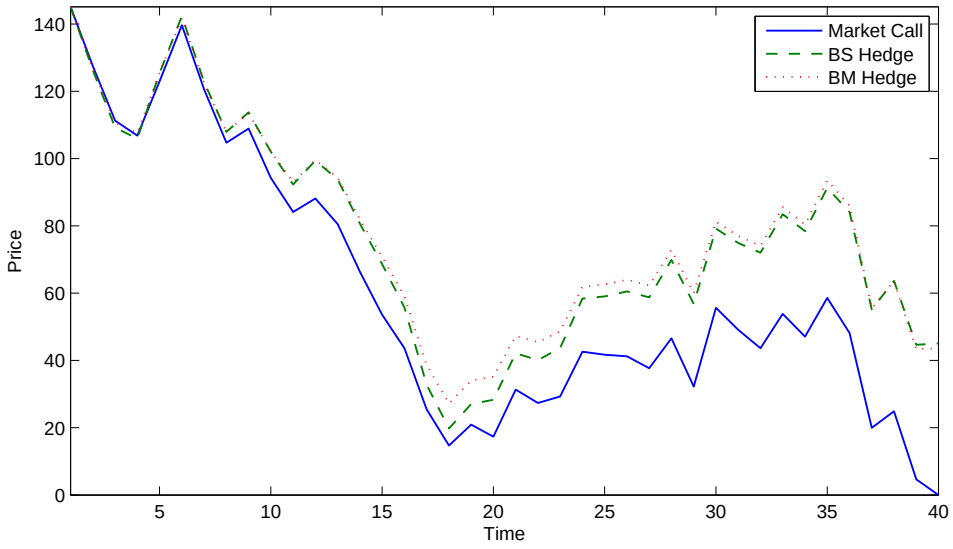

Figure 6.4: This figure displays two delta hedging portfolios together with the market call price. One has been hedged with the aid of the Black-Scholes delta and the other with the aid of the Brigo-Mercurio delta.

6.4.2 Hedging Scheme B

Next we apply the hedging scheme B, which means that we update the parameter σ in the Black-Scholes model and the parameters $\bar{\sigma}_1, \bar{\sigma}_2, \bar{\sigma}_3$ and $\lambda_1, \lambda_2, \lambda_3$ in the Brigo-Mercurio model every day. In Table 6.7 below we present the absolute hedging errors and in Figure 6.8 we present the relative hedging errors from hedging scheme B.

Period	Black-Scholes	Brigo-Mercurio
1	84.90	86.33
2	57.20	57.26
3	21.77	34.24
4	97.91	95.93
5	39.46	38.46
6	127.13	128.34
7	50.60	60.19
8	76.25	78.99
9	58.30	78.71
10	76.30	44.28
11	56.17	75.12
12	115.96	120.74

Table 6.7: The absolute hedging errors for each 1-month contract period when using hedging scheme B.

Period	Relative difference
1	+2%
2	0%
3	+57%
4	-2%
5	-3%
6	+1%
7	+19%
8	+4%
9	+35%
10	-42%
11	+34%
12	+4%

Table 6.8: The relative hedging errors for each 1-month contract period when using hedging scheme B.

We can conclude that the Brigo-Mercurio model is outperformed over the whole year by the Black-Scholes model. If one had used the Brigo-Mercurio model during the whole year the error would have increased by about 4% compared to Black-Scholes model.

However, we notice that from an investors point of view the hedging scheme B outperforms hedging scheme A in the Black-Scholes model. In fact, over the whole year the hedging error is reduced by 9% if one updates the parameter σ every day in the Black-Scholes model compared to keeping it constant over the whole contract period. In the Brigo-Mercurio model we can see that updating the parameters $\bar{\sigma}_1, \bar{\sigma}_2, \bar{\sigma}_3$ and $\lambda_1, \lambda_2, \lambda_3$ every day increased the error by 1% compared to keeping them fixed over the whole contract period.

Figure 6.5 displays the hedging portfolios using hedging scheme B in both the Black-Scholes model and the Brigo-Mercurio model during period 7. The call option that has been hedged has moneyness 102.5% at time zero i.e. at time zero the stock price is 2.5% above the strike price.

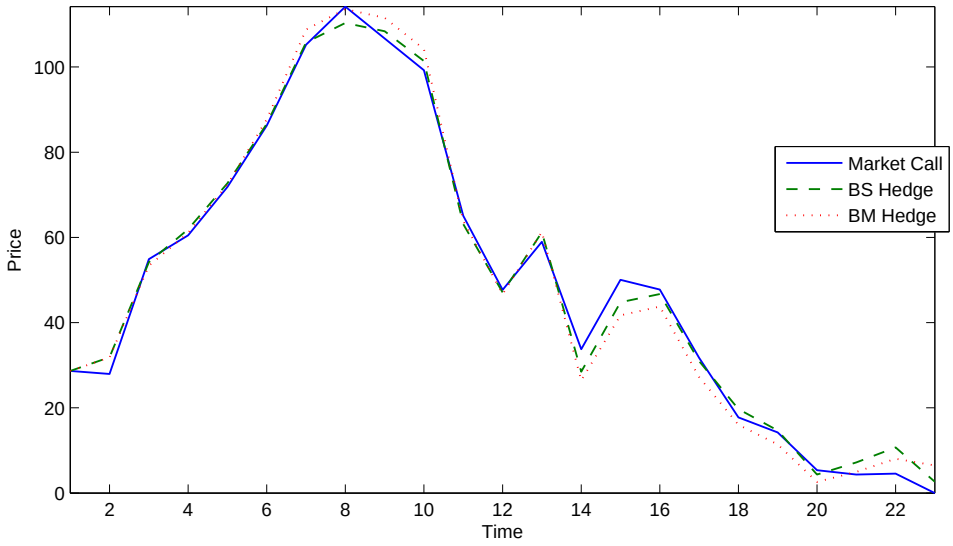

Figure 6.5: This figure displays two delta hedging portfolios together with the market call price during period 7. One has been hedged with the aid of the Black-Scholes delta and the other with the aid of the Brigo-Mercurio delta.

We conduct the same analysis on the 2-month options. The absolute hedging errors are presented in Table 6.9 below and in Table 6.10 we present the relative hedging errors for each period.

Period	Black-Scholes	Brigo-Mercurio
1	161.32	162.19
2	131.87	132.69
3	136.23	136.19
4	80.58	95.93
5	54.31	74.00

Table 6.9: The absolute hedging errors for each 2-month contract period when using hedging scheme B.

Period	Relative difference
1	+1%
2	+1%
3	0%
4	+19%
5	+36%

Table 6.10: The relative hedging errors for each 2-month contract period when using hedging scheme B.

Over the whole year the Black-Scholes model outperformed the Brigo-Mercurio model with hedging scheme B by approximately 7% for 2-month options.

Finally we test the hedging scheme B together with the alternative way of calibration (6.4). The absolute hedging errors for the 1-month contract periods is presented in Table 6.11 and the absolute hedging errors for the 2-month contract periods are presented in Table 6.12.

Period	Black-Scholes	Brigo-Mercurio
1	75.57	76.49
2	84.18	91.31
3	96.82	102.72
4	176.90	178.59
5	83.18	80.95
6	138.95	168.74
7	103.64	138.89
8	75.87	83.82
9	68.85	74.51
10	318.95	334.29
11	133.55	142.79
12	179.75	188.15

Table 6.11: The absolute hedging errors for each 1-month contract period when using hedging scheme B with the calibration (6.4).

Period	Black-Scholes	Brigo-Mercurio
1	163.02	189.96
2	107.55	112.83
3	121.13	108.34
4	193.81	223.90
5	236.08	324.16

Table 6.12: The absolute hedging errors for each 2-month contract period when using hedging scheme B with the calibration (6.4).

We can conclude that the hedging scheme B together with the calibration (6.4) is greatly outperformed by the other methods.

6.4.3 Varying ε and δ

Here we will investigate the effect of ε and δ on the hedging error using the Brigo-Mercurio model and hedging scheme A. As above we have $N = 3$ and $\bar{\sigma}$ is chosen as the optimal Black-Scholes parameter. We let $\delta = \varepsilon + 2/252$ and γ_i is the line segment between $\bar{\sigma}$ and $\bar{\sigma}_i$, $i = 1, 2, 3$, that is

$$\gamma_i(t) = \bar{\sigma} + (t - \varepsilon)\frac{\bar{\sigma}_i - \bar{\sigma}}{\delta - \varepsilon}, \quad t \in [\varepsilon, \delta], \quad i = 1, 2, 3.$$

Naturally, the largest ε we can have is $T-2$ where T is the time of maturity. In Table 6.13 we can see the result.

ε	Hedging error
1/252	77.05
2/252	77.14
3/252	77.21
4/252	77.28
5/252	77.35
6/252	77.41
7/252	77.48
8/252	77.54
9/252	77.60
10/252	77.66
11/252	77.72
12/252	77.77
13/252	77.82
14/252	77.86
15/252	77.90
16/252	77.93
17/252	77.96
18/252	77.98
19/252	77.99
20/252	78.00
21/252	78.01
22/252	78.01

(a) Period 1

ε	Hedging error
1/252	34.86
2/252	34.85
3/252	34.83
4/252	34.82
5/252	34.81
6/252	34.79
7/252	34.77
8/252	34.76
9/252	34.75
10/252	34.74
11/252	34.73
12/252	34.73
13/252	34.72
14/252	34.73
15/252	34.75
16/252	34.81
17/252	34.87
18/252	34.89
19/252	34.91
20/252	34.94
21/252	34.91
22/252	34.89

(b) Period 3

Table 6.13: The effect on the Hedging error when changing ε and δ.

From these two periods there seem to be no significant effect on the hedging error when varying ε and δ.

6.4.4 The sliding S_0 approach

In Section 6.4.2 we concluded that when recalibrating the parameters every day the Black-Scholes model outperformed the Brigo-Mercurio model over the whole year for both 1-month contracts and 2-month contracts. We argued that we could calculate delta each day by differentiating the relation (5.12). However, by doing this we loose the dynamics of the Brigo-Mercurio model. Next we will try using the solution to the PDE (6.1) to calculate delta each day. By doing so we can utilize the local volatility function (5.8) which keeps the dependence on S_0 during the whole time to maturity, where S_0 denotes the stock price at the time we choose to have as the starting point in time.

We will still calibrate the parameters $\bar{\sigma}_1, \bar{\sigma}_2, \bar{\sigma}_3$ and $\lambda_1, \lambda_2, \lambda_3$ every day using (6.3) but we calculate the Brigo-Mercurio delta each day by numerically differentiating the PDE-solution. To be more precise, when we solve the PDE (6.1) we must discretize the time and in particular choose a starting time. Suppose we have the same time grid as previously in this chapter, $0 = t_0 < t_1 < ... < t_n = T$, where each time point represent one day of an option contract that matures at time T. If $m \in \{0, ..., n\}$ is fixed and we currently are at some time t_i, $0 \leq i \leq n$, we solve the PDE by discretizing the time from time t_0, if $i \leq m$, and from t_{i-m}, if $i \geq m+1$. Correspondingly, we let $S_0 = S(0)$, if $i \leq m$, and $S_0 = S(t_{i-m})$, if $i \geq m+1$.

This method of hedging by sliding S_0 m days behind the present time will in the sequel be denoted by *sliding*(m). Note that the case *sliding*(T) is equivalent to keeping S_0 fixed during the whole contract period and this hedging strategy is the first we will investigate.

In Table 6.14 we present the absolute hedging errors from the *sliding*(T) hedging scheme for the 1-month call options and in Table 6.15 we present the corresponding errors for the 2-month call options. The hedging errors are compared with the hedging errors in the Black-Scholes model from hedging scheme B. We can conclude that over the whole year the Brigo-Mercurio model outperforms the Black-Scholes model by 4% on 1-month options. However, on 2-month options the Black-Scholes model outperformes the Brigo-Mercurio model by 8%. It is mainly Period 5 that contributes to this large error.

Period	Black-Scholes	Brigo-Mercurio
1	84.88	75.66
2	57.22	53.88
3	21.77	31.84
4	97.97	98.55
5	39.42	46.96
6	127.10	120.30
7	50.46	49.69
8	76.26	90.48
9	58.32	41.41
10	76.29	60.56
11	56.17	46.47
12	115.77	114.32

Table 6.14: The absolute hedging errors for each 1-month contract. The hedging errors in the Brigo-Mercurio model with the $sliding(T)$ hedging scheme is compared with the hedging errors in the Black-Scholes model from hedging scheme B.

Period	Black-Scholes	Brigo-Mercurio
1	161.32	164.95
2	131.87	145.56
3	136.23	131.56
4	80.58	81.32
5	54.31	91.74

Table 6.15: The absolute hedging errors for each 2-month contract. The hedging errors in the Brigo-Mercurio model with the $sliding(T)$ hedging scheme is compared with the hedging errors in the Black-Scholes model from hedging scheme B.

We can ask the question whether or not it is sensible to keep S_0 fixed during the whole time to maturity. Maybe it is more sensible to only look back 5 or 10 days in time i.e. to use the $sliding(5)$ or the $sliding(10)$ hedging scheme defined above. This is what we will investigate next and we begin by testing the $sliding(5)$ scheme.

The results from the $sliding(5)$ hedging scheme is presented in Tables 6.16 and 6.17 together with the Black-Scholes hedging error from hedging scheme B. This strategy seems to work well on some periods but extremely bad on others and over the whole year the Black-Scholes model outperformed the Brigo-Mercurio model by 8% on 1-month options. For the 2-month options we can conclude that the strategy works well on Period 1-3 but extremely bad on Period 4 and 5 and over the whole year the Black-Scholes model would have outperformed the Brigo-Mercurio model by 15%.

Period	Black-Scholes	Brigo-Mercurio
1	84.88	68.99
2	57.22	57.34
3	21.77	39.03
4	97.97	99.00
5	39.42	48.83
6	127.10	123.99
7	50.46	61.34
8	76.26	87.54
9	58.32	63.35
10	76.29	86.46
11	56.17	52.38
12	115.77	150.51

Table 6.16: The absolute hedging errors for each 1-month contract. The hedging errors in the Brigo-Mercurio model with the *sliding*(5) hedging scheme is compared with the hedging errors in the Black-Scholes model from hedging scheme B.

Period	Black-Scholes	Brigo-Mercurio
1	161.32	163.38
2	131.87	139.60
3	136.23	131.37
4	80.58	115.05
5	54.31	114.18

Table 6.17: The absolute hedging errors for each 2-month contract. The hedging errors in the Brigo-Mercurio model with the *sliding*(5) hedging scheme is compared with the hedging errors in the Black-Scholes model from hedging scheme B.

Even though the above strategy seems fruitless we are interested in seeing what happens if we slide S_0 10 days behind present time instead of 5 days. The results are presented in Tables 6.18 and 6.19 and again compared with the hedging errors in the Black-Scholes model from hedging scheme B. There is not much difference compared to when looking back 5 days. The Black-Scholes model still outperformed the Brigo-Mercurio model by about 8% for 1-month call options and by about 15% for 2-month call options.

Period	Black-Scholes	Brigo-Mercurio
1	84.88	67.36
2	57.22	59.40
3	21.77	32.83
4	97.97	97.01
5	39.42	48.99
6	127.10	127.37
7	50.46	65.27
8	76.26	88.60
9	58.32	70.14
10	76.29	89.62
11	56.17	49.05
12	115.77	140.44

Table 6.18: The absolute hedging errors for each 1-month contract. The hedging errors in the Brigo-Mercurio model with the *sliding*(10) hedging scheme is compared with the hedging errors in the Black-Scholes model from hedging scheme B.

Period	Black-Scholes	Brigo-Mercurio
1	161.32	158.89
2	131.87	134.99
3	136.23	131.05
4	80.58	120.42
5	54.31	102.51

Table 6.19: The absolute hedging errors for each 2-month contract. The hedging errors in the Brigo-Mercurio model with the *sliding*(10) hedging scheme is compared with the hedging errors in the Black-Scholes model from hedging scheme B.

From these investigations it seems as the best strategy is *sliding*(T) i.e. to keep S_0 fixed and not to change it over time. With this strategy the Brigo-Mercurio model outperformed the Black-Scholes model by about 4% for 1-month options. However on 2-month options the Black-Scholes model with hedging scheme B outperformed the Brigo-Mercurio model.

Now consider buying a 2-month call option when there is only one month left to maturity. This could be seen as entering into a 1-month call option with the same strike price as the 2-month call option. Let t^* denote the point in time when there is only one month left to maturity on a 2-month call option. We then hedge in the same fashion as above, with $S_0 = S(t^*)$ kept fixed. The results are presented in Table 6.20 and we compare with the hedging error in the Black-Scholes model from hedging scheme B.

Period	Black-Scholes	Brigo-Mercurio
1	61.81	69.47
2	90.94	89.96
3	118.93	113.77
4	44.99	48.37
5	60.46	86.01

Table 6.20: The absolute hedging errors for each 2-month contract compared with the error in the Black-Scholes model from hedging scheme B.

Over the whole year, this hedging strategy resulted in the Black-Scholes model outperforming the Brigo-Mercurio model by about 7%.

Note that two call options issued at the same moneyness, but at different points in time will most likely be different contracts due to possible differences in strike prices. For example, a 2-month call option issued at the money will at time t^* not necessarily be the same contract as a 1-month call option issued at the money at time t^*.

What if it was possible to enter into a 2-month call option, at time t^*, with a strike price such that the call option is at the money at time t^*. In theory, this contract is equivalent to a 1-month call option issued at the money at time t^*. However, in practice it might not be possible to buy such a contract, but it is possible by interpolation to construct one from market prices. It is interesting to investigate whether or not that kind of contract resembles the 1-month call issued at the money at time t^*.

In Figure 6.6 we compare the prices of a 2-month call option entered at the money at time t^* in Period 1 and a 1-month call option issued at the money in Period 2. We can clearly see that they are quite similar.

It is also interesting to investigate the hedging errors for the 2-month call options entered at time t^* with the same strike prices as for the 1-month call options issued at t^*. The corresponding hedging errors for the 1-month contracts issued at t^* are presented above in Table 6.14 (period 2,4,6,8 and 11). The results from hedging the 2-month call options from t^* to maturity using the same hedging strategy as above, with $S_0 = S(t^*)$ kept fixed, is presented in Table 6.21.

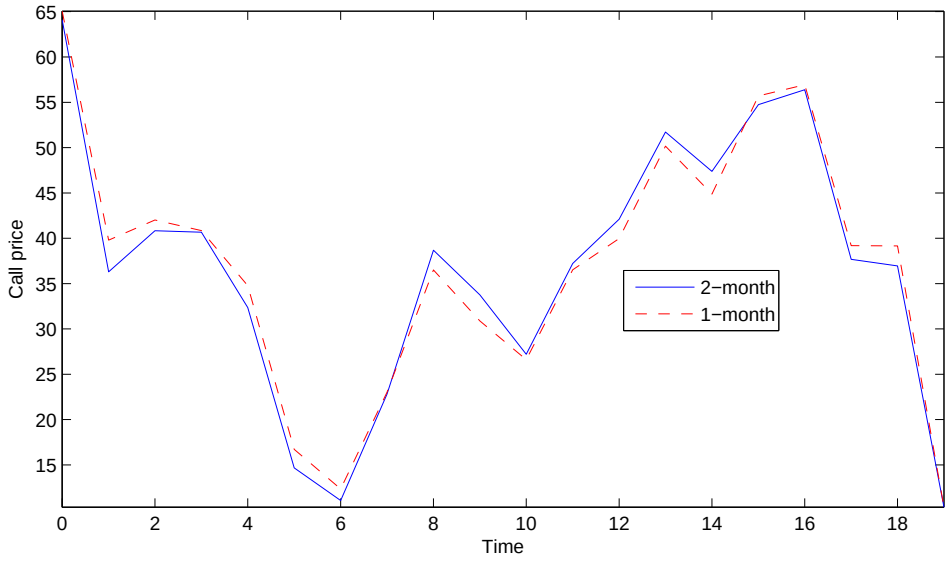

Figure 6.6: This figure compares the prices of a 2-month call option bought at the money at time t^* in Period 1 and a 1-month call option issued at the money in Period 2.

Period	Black-Scholes	Brigo-Mercurio
1	50.75	45.65
2	117.16	118.92
3	106.92	108.55
4	65.20	73.01
5	47.88	47.75

Table 6.21: The absolute hedging errors for each interpolated 2-month contract between t^* and maturity. The error in the Black-Scholes model are from hedging scheme B.

We must conclude that even though the call prices, at least in Figure 6.6, were similar there are significant differences in the hedging errors between hedging the 2-month call options from t^* to maturity compared with hedging the 1-month call options issued at t^*. In fact, over the whole year, in the Black-Scholes model the difference is about 7% and in the Brigo-Mercurio model the difference is about 6%.

Furthermore, when entering the 2-month contracts at time t^* we can conclude from Table 6.21 that the Black-Scholes model outperforms the Brigo-Mercurio model by about 2%. That is not very surprising since the Black-Scholes model outperforms the Brigo-Mercurio model over the particular periods 2,4,6,8 and 11 (recall Table 6.14), although the Brigo-Mercurio model outperformed the Black-Scholes model over the whole year.

Chapter 7

Conclusions

The aim of this thesis was to investigate the Brigo-Mercurio log-normal mixture option pricing model and to conclude whether or not it had any effect in reducing the hedging error compared with the Black-Scholes model.

In Section 6.4.1 we found that under the hedging scheme A the Brigo-Mercurio model outperformed the Black-Scholes model over the whole year with approximately 3% on 1-month call options whilst on 2-month call options the Black-Scholes model outperformed the Brigo-Mercurio model by approximately 1%.

Under the hedging scheme B in Section 6.4.2 we found that the Brigo-Mercurio model was outperformed by the Black-Scholes model by approximately 4% for 1-month call options. However for 2-month call options we concluded that the Brigo-Mercurio model outperformed the Black-Scholes model by approximately 1% over the whole year. We concluded that using hedging scheme B was preferable to hedging scheme A in the Black-Scholes model for both 1-month and 2-month call options. However in the Brigo-Mercurio model hedging A was preferable to hedging scheme B for both 1-month and 2-month call options.

Further, we tested an alternative way of calibrating the parameters, namely by minimizing the absolute distance between the hedging portfolio and the market price of the call. This approach proved to be more or less useless with the exception of one or two periods. We also concluded, in Section 6.4.3, that the hedging error under hedging scheme A was not very sensitive to changes in ε and δ.

However, we found in Section 6.4.4 that it might be a good idea to use the PDE-solution to calculate delta every day with recalibrated parameters and S_0 fixed. This utilizes the dynamics from the Brigo-Mercurio model and ultimately, for 1-month call options, it proved to outperform the Black-Scholes model under hedging scheme B by around 4% over the whole year. Unfortunately, for 2-month call options the Black-Scholes model outperformed this strategy by around 8%.

We also considered the method of sliding the starting point S_0 a few days behind the present time instead of always using the starting point at time zero. We considered both 5 and 10 days behind but both of these produced larger hedging errors than considering the starting point at time zero fixed over the whole period.

All in all, after extensive investigation of the hedging error of various hedging strategies, we can not conclude that any strategy is better than the Black-Scholes model under hedging scheme B. We can only outperform this strategy on 1-month options and not on 2-month options. We cannot find any pattern for when a strategy is better than the Black-Scholes model under hedging scheme B. However, we feel that further investigation should be conducted with more and different market prices and especially options with longer running time.

Bibliography

[1] F. Mercurio D. Brigo. Displaced and mixture diffusions for analytically-tractable smile models. In S.R. Pliska A.C.F. Vorst H. Geman, D.B. Madan, editor, *Mathematical Finance - Bachelier Congress 2000*. Springer, 2000.

[2] Euro stoxx 50. `http://www.stoxx.com/indices/index_information.html?symbol=SX5P`. Read 2012-02-13.

[3] R.A. Davis P.J. Brockwell. *Time Series: Theory and Methods*. Springer, 1991.

[4] R.T. Gregory D.M. Young. *A Survey of Numerical Mathematics*, volume 2. Addison-Wesley, 1973.

[5] R.J. Ritchey. Call option valuation for discrete normal mixtures. *Journal of Financial Research*, 13:285–296, 1990.

[6] C.P. Thomas W.R. Melick. Recovering an asset's implied pdf from option prices: An application to crude oil during the guld crisis. *Journal of Financial and Quantitative Analysis*, 32:91–115, 1997.

[7] C. Guo. An application of the chi-squared goodness-of-fit test to discrete common stock returns. *The Financial Review*, 33:81–92, 1998.

[8] M. Chesney M. Jeanblanc, M. Yor. *Mathematical Methods for Financial Markets*. Springer, 2009.

[9] Euro interbank offered rate. `http://www.euribor-ebf.eu/assets/files/Euribor_tech_features.pdf`. Read 2012-02-13.

[10] Eurex contract specifications. `http://www.eurexchange.com/trading/products/IDX/DAX/ODAX_en.html`. Read 2012-02-13.